SANDIA REPORT
SAND2020-11695
Printed October, 2020

Sandia National Laboratories

FOSWEC dynamics and controls test report

Ryan G. Coe, Giorgio Bacelli, Dominic Forbush, Steven J. Spencer, Kevin Dullea, Bret Bosma, Pedro Lomonaco

Prepared by
Sandia National Laboratories
Albuquerque, New Mexico 87185
Livermore, California 94550

Issued by Sandia National Laboratories, operated for the United States Department of Energy by National Technology & Engineering Solutions of Sandia, LLC.

Available to DOE and DOE contractors from

U.S. Department of Energy
Office of Scientific and Technical Information
P.O. Box 62
Oak Ridge, TN 37831

Telephone: (865) 576-8401
Facsimile: (865) 576-5728
E-Mail: reports@osti.gov
Online ordering: http://www.osti.gov/scitech

Available to the public from

U.S. Department of Commerce
National Technical Information Service
5301 Shawnee Road
Alexandria, VA 22312

Telephone: (800) 553-6847
Facsimile: (703) 605-6900
E-Mail: orders@ntis.gov
Online order: https://classic.ntis.gov/help/order-methods

ABSTRACT

This report describes the testing of a model scale wave energy converter. This device, which uses two “flaps” that pivot about a central platform when excited by waves, has a natural frequency within the range of the waves by which it is excited. The primary goal of this test was to assess the degree to which previously developed modeling, experimentation, and control design methods could be applied to a broad range of wave energy converter designs. Testing was conducted to identify a dynamic model for the impedance and excitation behavior of the device. Using these models, a series of closed loop tests were conducted using a causal impedance matching controller. This report provides a brief description of the results, as well as a summary of the device and experimental design. The results show that the methods applied to this experimental device perform well and should be broadly applicable.

CONTENTS

LIST OF FIGURES

LIST OF TABLES

1. INTRODUCTION

This report summarizes the design and execution of a wave tank test of the floating oscillating surge wave energy converter (FOSWEC) at the Oregon State University (OSU) O.H. Hinsdale Wave Research Laboratory (HWRL) Directional Wave Basin (DWB). The FOSWEC was previously tested to produce model validation data for the WEC-Sim code [10, 4, 11]. The device design was updated to improve closed loop control performance.

The testing campaign that is the focus of this report has the following high-level goals:

1. Show that engineering tools and methods applied to the WaveBot in previous tests (see, e.g., [5, 2, 6, 3]) are equally applicable to the FOSWEC, and therefore more broadly applicable to a wide range of wave energy devices. These methods include:
    a) Hardware and data acquisition (DAQ) system design
    b) System identification (SID)
    c) Control design
    d) Control performance evaluation
2. Produce an open-source dataset to be hosted on `https://mhkdr.openei.org`
3. Ensure the proper function of the FOSWEC hardware for usage in future testing campaigns by OSU

The subsequent sections of this report provide an overview of the FOSWEC and experimental design (Section 2), system identification (SID) testing results (Section 3.1), and closed-loop control testing results (Section 3.2). Additionally, appendices provide the testing procedure, test log, data structure for files available from `https://mhkdr.openei.org`, real-time control software details, bench-testing results, and a summary of previously completed testing of the FOSWEC under the WEC-Sim program.

2. EXPERIMENTAL SET UP

2.1. FOSWEC device

The FOSWEC is a dual flap wave energy device designed for testing at the DWB. The FOSWEC device was previously designed and tested at the DWB as part of an effort to validate the open-source model WEC-Sim [10, 4, 11]. [1] The FOSWEC was originally considered to be a 1:33 scale device, however, for the current tests, no fixed relative scale is used (i.e., the WEC is considered to be scaled for the basin's wave environment in which it operates).

To perform testing focused on system identification and closed loop control, a series of design modifications were made to the FOSWEC. These changes were generally targeted to improve the performance of the power take-off (PTO) system in terms of closed loop control. Appendix F summarizes changes made to the design for the current testing campaign. The updated FOSWEC device is referred to herein as the "FOSWEC v2."

The physical parameters for current FOSWEC v2 design are listed in Table 2-1. Figure 2-1 shows a CAD rendering and labels for sensors and features of the FOSWEC v2. The device has two flaps that are hinged to pivot about shafts mounted to a central platform. The central platform comprises a water-tight DAQ housing and four surface piercing spars that provide buoyancy. The flaps are driven by two identical belt drive systems with a 3.75:1 gear ratio. Each drive train employs an AMC DPEANIU-040A400 motor drive and an Allied Motion MF0150025-C0X permanent magnet synchronous motor. Figure 2-2 shows a simplified diagram of the FOSWEC v2 with some key dimensions.

[1] Appendix F provides details and some summarized results from this previous test for easy reference.

Table 2-1 FOSWEC v2 device parameters.

Parameter	Value
Mass, m [kg]	263 kg
Length, ℓ [m]	1.44
Beam (width), w [m]	1.63
Draft, T [m]	< 1.24
Flap natural freq., f_n [Hz]	0.35
Power, motor	208 VAC, 30 A
Power, DAQ	110 VAC, < 10 A
Gear ratio, N	3.75
Motor pulley teeth	20
Flap pulley teeth	75
Motor torque constant, k_τ [Nm/A]	0.943
Motor winding resistance, R [Ω]	1.082

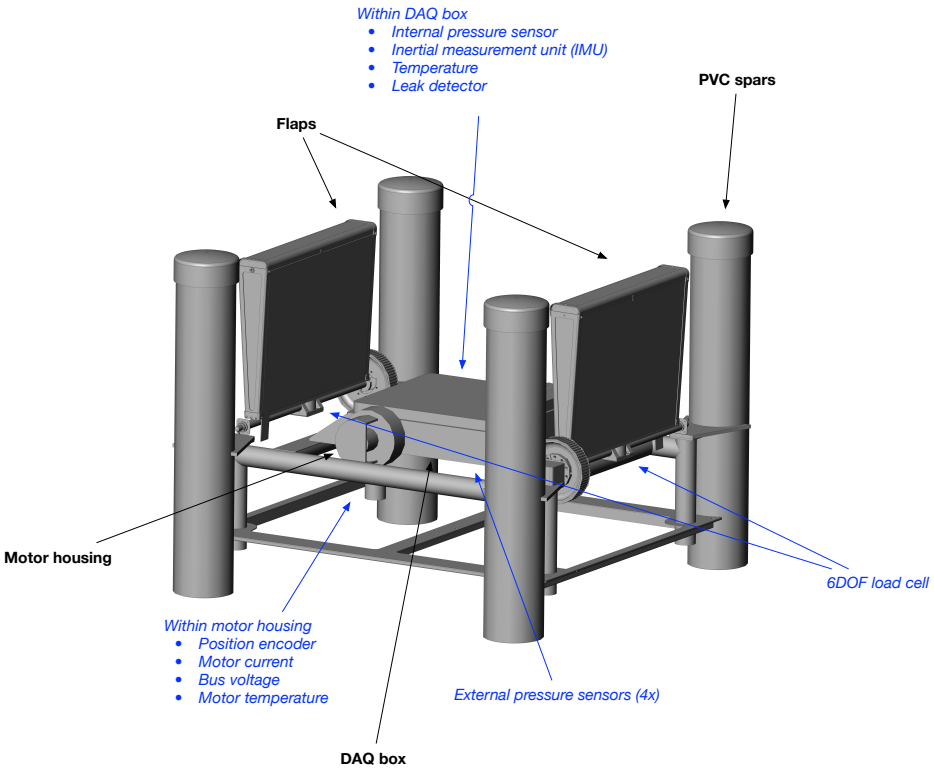

Figure 2-1 FOSWEC v2 CAD rendering showing components and sensor locations.

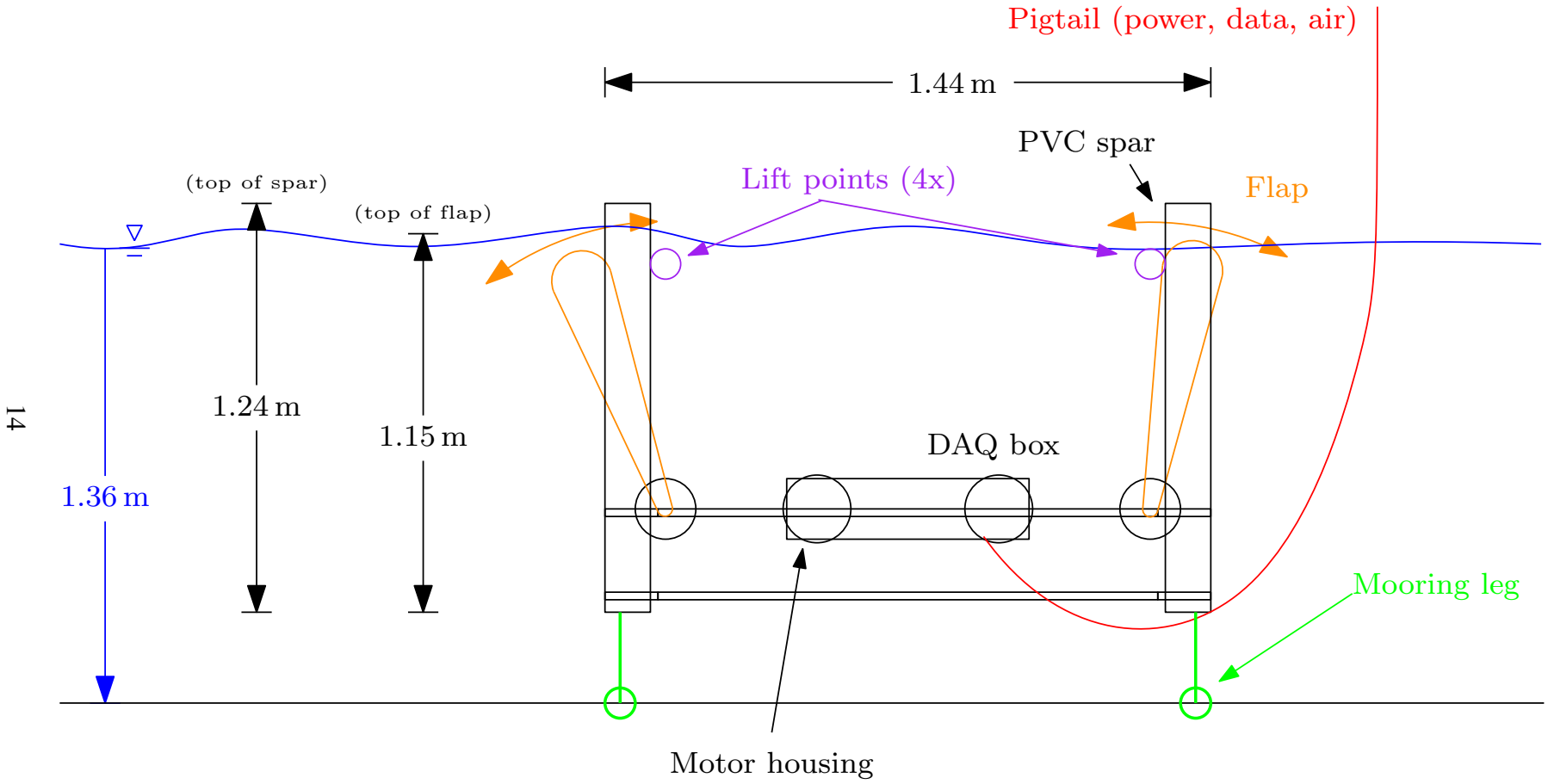

Figure 2-2 FOSWEC v2 simplified diagram.

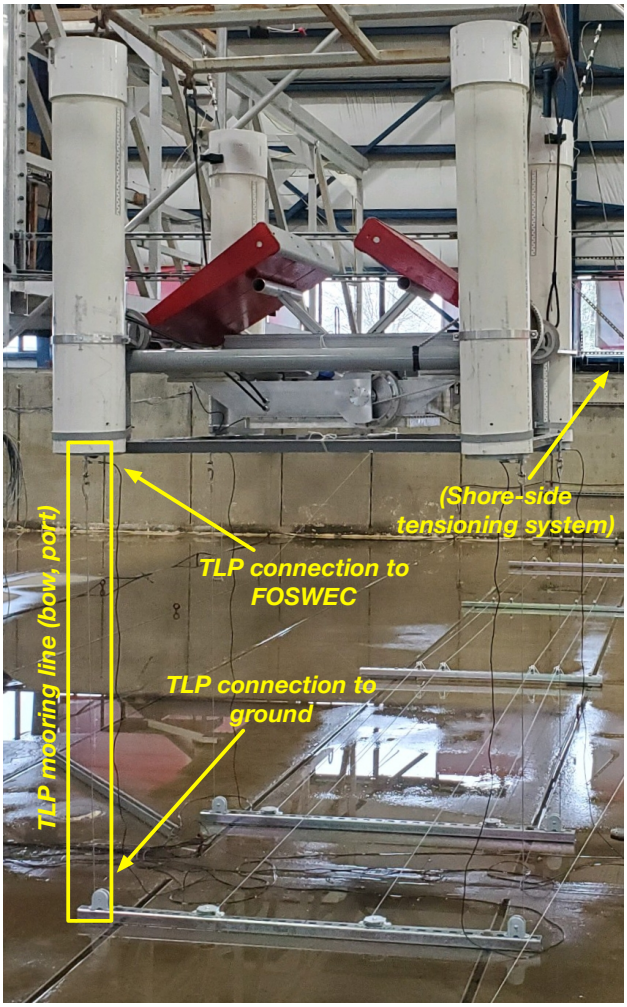

Figure 2-3 FOSWEC tension leg platform (TLP) mooring system (note that Figure 2-4 provides a diagram of the TLP system).

2.1.1. Mooring

The FOSWEC v2 uses a tension leg platform (TLP) mooring system. An annotated photograph of the FOSWEC v2's TLP system is shown in Figure 2-3. With no added ballast and the spars fully filled with foam, the FOSWEC v2 has roughly 540 N of excess buoyancy when submerged to a point where the flaps are just below the free surface. Thus, for a four leg TLP system, each leg sees 135 N of tension. The hydrostatic stiffness in heave of the FOSWEC v2 (assuming only the effect from the four spars, an under-estimate) is 1.4 kN/m. Assuming that the FOSWEC v2 is subjected only to planar waves with no off angle headings, the mooring system should therefore remain taught in waves up to roughly 0.4 m in amplitude.

The TLP system is tensioned via an on-shore system. This allows for the TLP system to be loosened and for the FOSWEC v2 to be lifted out of the water during breaks from testing (e.g., at night). To avoid an over-constrained system, the port and starboard lines from the bow and aft are tensioned by a single winch, respectively. This system is depicted in Figure 2-4.

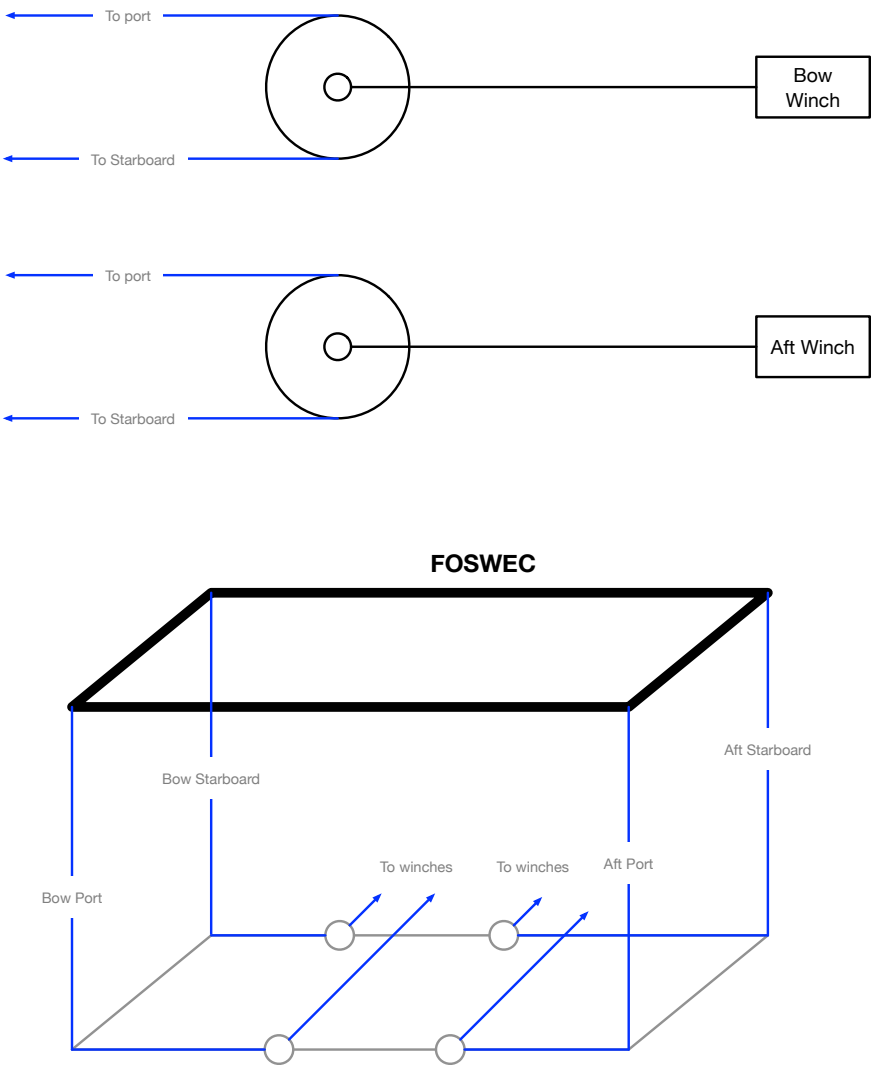

Figure 2-4 FOSWEC v2 tension leg platform (TLP) mooring tensioning system. TLP cables shown in blue. Upper half of diagram shows the shore-side tensioning system. Lower half of diagram (correlating to Figure 2-3) shows the lower frame of the FOSWEC v2 and TLP legs.

2.1.2. Data acquisition and control

As shown in Figure 2-5, the wave tank test utilized two DAQ systems:

- **SNL** - The Sandia DAQ system utilizes an EtherCAT based acquisition and control network run with a Simulink Real-time Speedgoat target. The acquisition/control network includes Beckhoff acquisition cards and AMC motor controllers with EtherCAT fieldbus connectivity. A detailed diagram of the FOSWEC v2 instrumentation and Sandia DAQ system is shown in Figure 2-5. Within Figure 2-5, two Sandia DAQ subsystems are shown: a "shore" and "disconnect/sync." system, located at the basin edge, and a "dry box" system, which is located on board the FOSWEC v2. The physical layout of this system is depicted in Figure 2-6.
- **HWRL** - The HWRL DAQ system, shown on the right-hand side of Figure 2-5, collects wave probe signals and wave maker data. Additionally, HWRL utilizes a PhaseSpace system to measure the rigid-body movement of the FOSWEC v2 platform and also measure mooring tensions.
  - Wavemaker trigger, displacement, and surface elevation at wave-board 15 of the wave machine.
  - PhaseSpace was mounted on a fixed structure at the center of the basin. The structure was supported by 4 cylindrical columns attached to the basin floor, forming a 6 m $\times$ 6 m measurement section (see Figure 2-10).
  - Eight wave gauges mounted on the PhaseSpace frame to measure the wave conditions around the device (see Figure 2-12 and Figure 2-13)
  - Four submersible load cells were installed at the mooring line attachments
  - Video and digital cameras to assist in test execution

The two DAQ systems were synchronized by simultaneously recording both a random noise signal and a 1 Hz sine wave signal (both $\pm$5 V), which can be aligned in post-processing. These synchronization signals were generated by HRWL. Additionally, Sandia captured the wave maker start/stop TTL signal.

Figure 2-6 shows a diagram of the layout for the DAQ and FOSWEC v2 systems within the DWB. The systems in Figure 2-6 correlate with those illustrated in detail in Figure 2-5. The external equipment is located on the south edge of the basin; this includes the "Shore" system (with the host PC operated by the personnel conducting the test), the "Disconnect/Sync." system, and the HRWL DAQ. Note that all power is received on the shore by the "Disconnect/Sync." system, which includes a lock-ready blade switch, absence of voltage (AVT) tester, and emergency stop ("E-stop") button. To power the FOSWEC v2, the "Disconnect/Sync" system receives 208 VAC and 110 VAC power. The 208 VAC power is passed through a fused disconnect switch and relayed to the FOSWEC v2. Additionally, the Panduit Verisafe AVT measures this 208 VAC circuit. The 110 VAC power is converted to 24 VDC (10 A) and relayed to the FOSWEC v2.

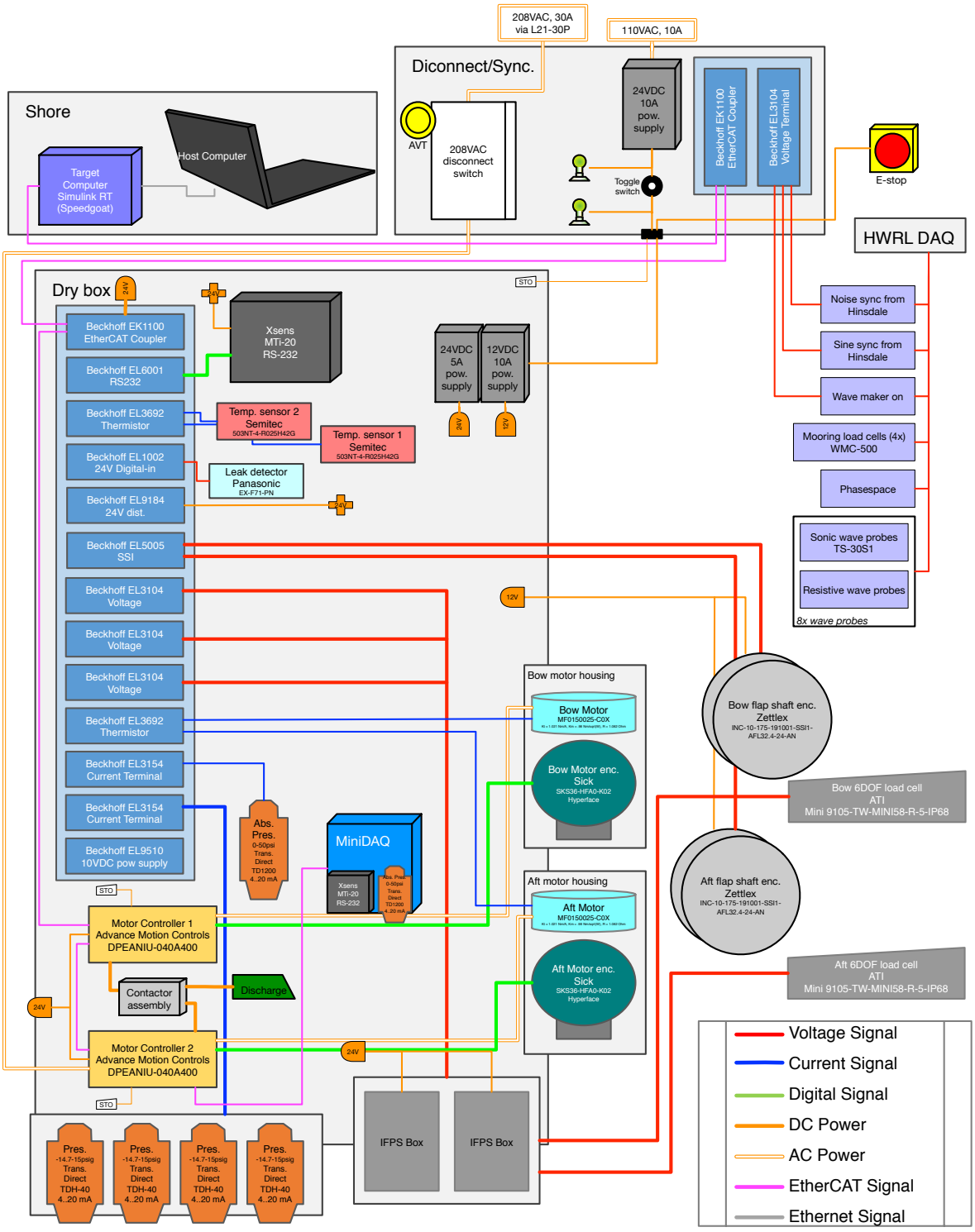

Figure 2-5 FOSWEC v2 measurements and Sandia DAQ system. Note that Figure 2-6 provides a physical layout of the system within the basin.

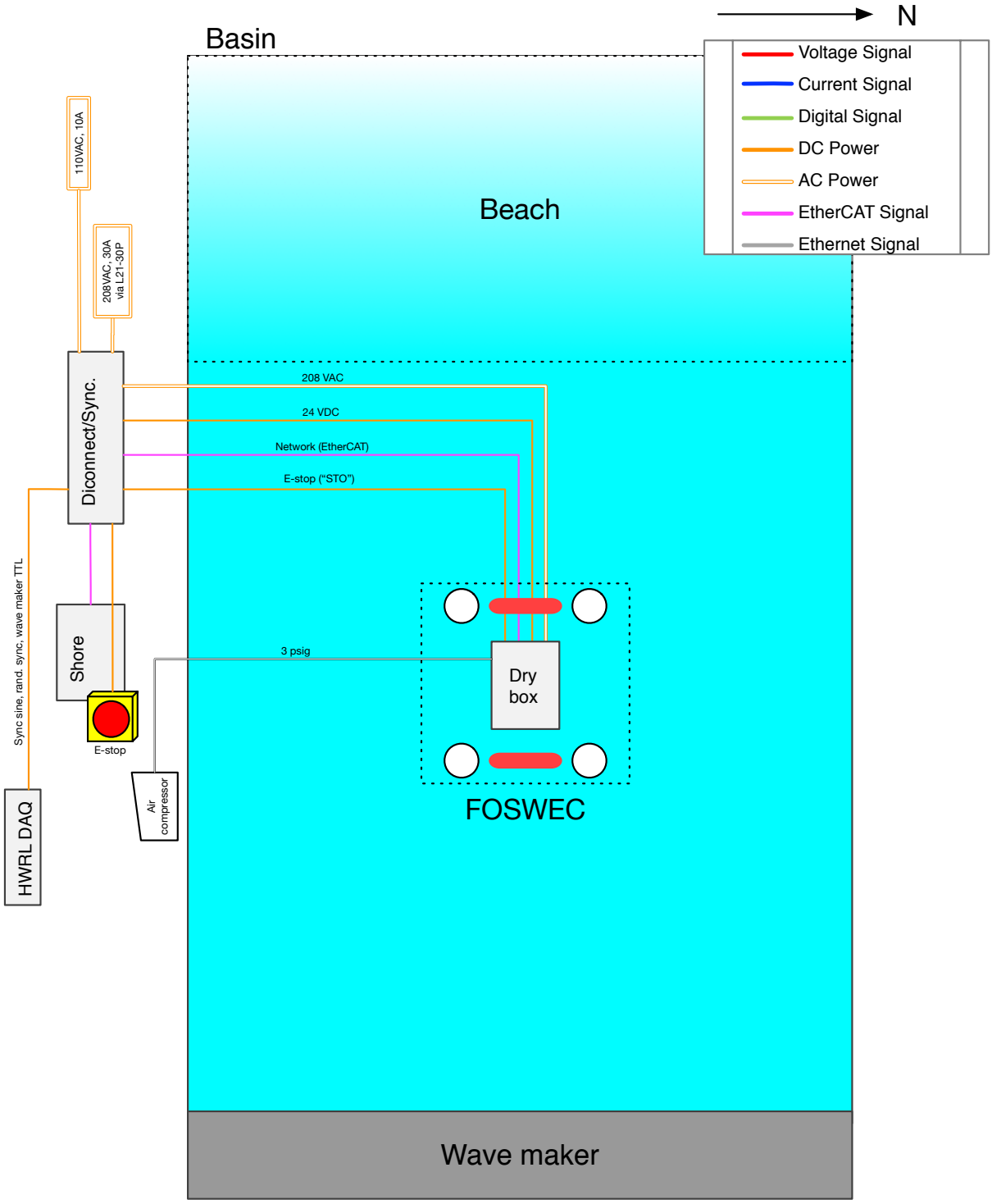

Figure 2-6 FOSWEC v2 DAQ/electronics layout.

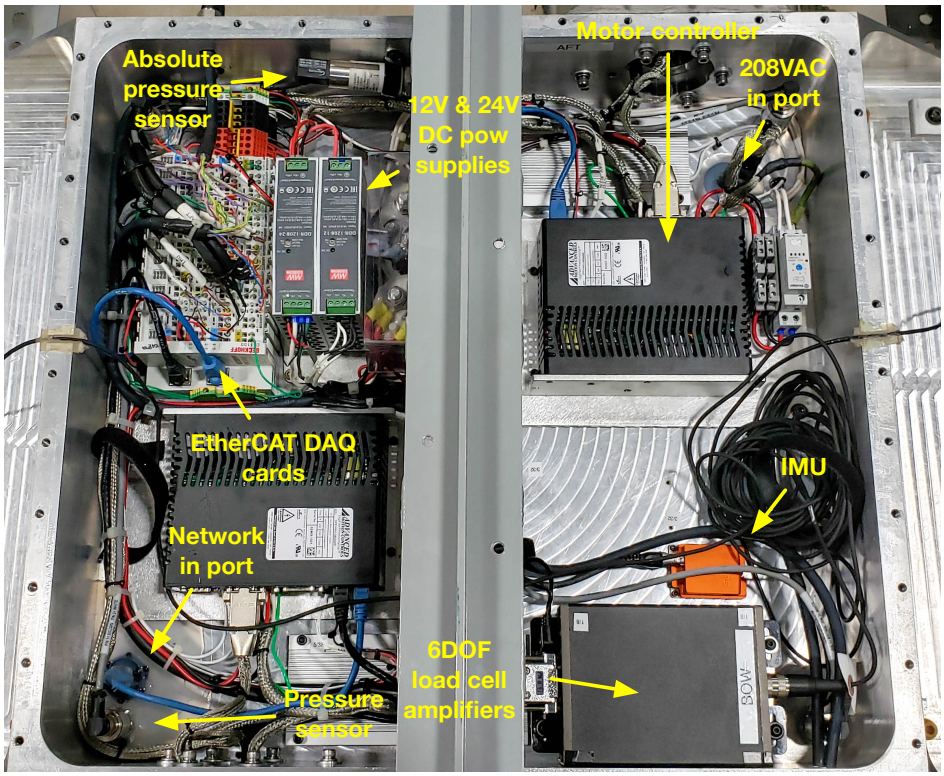

Figure 2-7 FOSWEC v2 housing internal photo.

Figure 2-7 shows an internal photo of the FOSWEC v2's on-board DAQ housing ("Dry box" in Figure 2-5). This box includes all data acquisition and control systems on-board the FOSWEC v2. Additionally, a number of sensors are housed in the "Dry box." These include five pressure sensors, 4 of which are relative sensors (Transducer Direct TDH-40) to measure the external water pressure and 1 of which is an absolute sensor (Transducer Direct TD1200) to measure the internal hull pressure. Two Semitec 503NT-4-R025H42G temperature sensors (thermistors) are included in the hull along with a Panasonic EX-F71-PN leak detection sensor. The "Dry box" also houses a Xsens MTi-20 RS-232 inertial measurement unit (IMU). To process the signals from 6-DOF load cells mounted at the aft and bow flaps (ATI Mini 9105-TW-MINI58-R-5-IP68), the "Dry box" also includes two amplifier/signal conditioner units ("IFPS Box" in Figure 2-5).

The two AMC motor drives both include power rectifiers, but only the aft drive rectifier is used. Because this rectifier serves both of the drives, a substantial inrush current can occur when the device is powered on. To avoid this issue, a timed relay and motor contactor are employed to delay powering of the bow drive until the capacitors of the bow drive are at least partially charged.

Figure 2-8 shows the "disconnect box" system ("Disconnect/Sync." in Figure 2-5) for the FOSWEC v2. This includes switching and indicators for both low (24 VDC) and high (208 VAC) power. The status of the 24 VDC power is indicated by an LED. The status of the 208 VAC power is indicated by an AVT (Panduit VS-AVT-C02-L03). Additionally, the disconnect box houses data acquisition cards for acquiring synchronization signals.

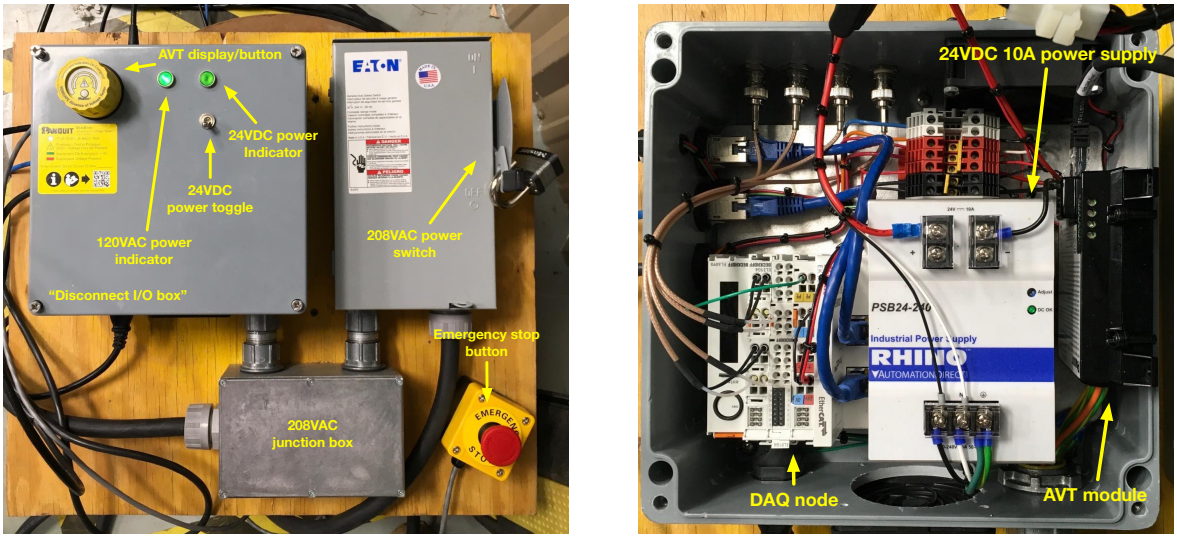

(a) Complete disconnect system. **(b) Inside of disconnect I/O box.**

Figure 2-8 Photos of FOSWEC v2 "disconnect box."

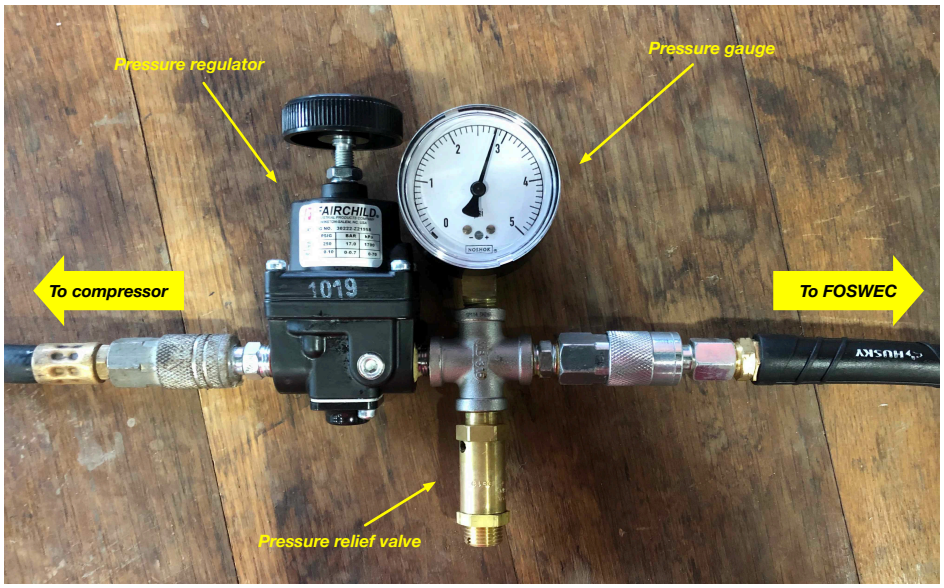

Figure 2-9 FOSWEC v2 pressure system.

2.1.3. Water-tight housing

All connectors for the water-tight DAQ housing are IP69 rated. Additionally, to reduce the likelihood of water ingress, the DAQ housing was pressurized to roughly 3 psig (20.7 kPa). The pressure is provided via an air hose, which connects to an air compressor on the tank shore via a pressure regulation assembly (see Figure 2-9). The system comprises a precision compressed air regulator, a fast-acting pressure-relief valve set to 5 psig (35 kPa), and a dial pressure gauge. The pressure regulator has a maximum regulating pressure of 10 psig (69 kPa), regulating accuracy of $\pm 0.2\%$, and a maximum pressure of 250 psig (1724 kPa). At a depth of 1 m, the hydrostatic pressure outside the hull is 1.4 psig (9.8 kPa).

2.1.4. PhaseSpace

Figure 2-10 shows the key components of the PhaseSpace system used for motion capture. This system provides an additional motion measurement to the FOSWEC v2's onboard IMU (see Figure 2-5). The origin of the PhaseSpace coordinate axis definition square for the SandiaFOSWEC project in HWRL coordinates is as follows: $[x = 19.088, y = 0.455, z = 1.935]$ m.

All surveys and instrument locations are reported using the HWRL coordinate system. The HWRL coordinate system is defined as follows:

- The x-axis is the cross-shore coordinate. Its origin ($x = 0$) is at a vertical plane that best fits the face of the wavemaker piston when it is neutrally positioned. The x-axis is measured in meters and positive onshore (away from the wavemaker).
- The z-axis is the vertical coordinate. The z-axis origin ($z = 0$) is at the average elevation of the tank floor. The z-axis is measured in meters and positive upwards.

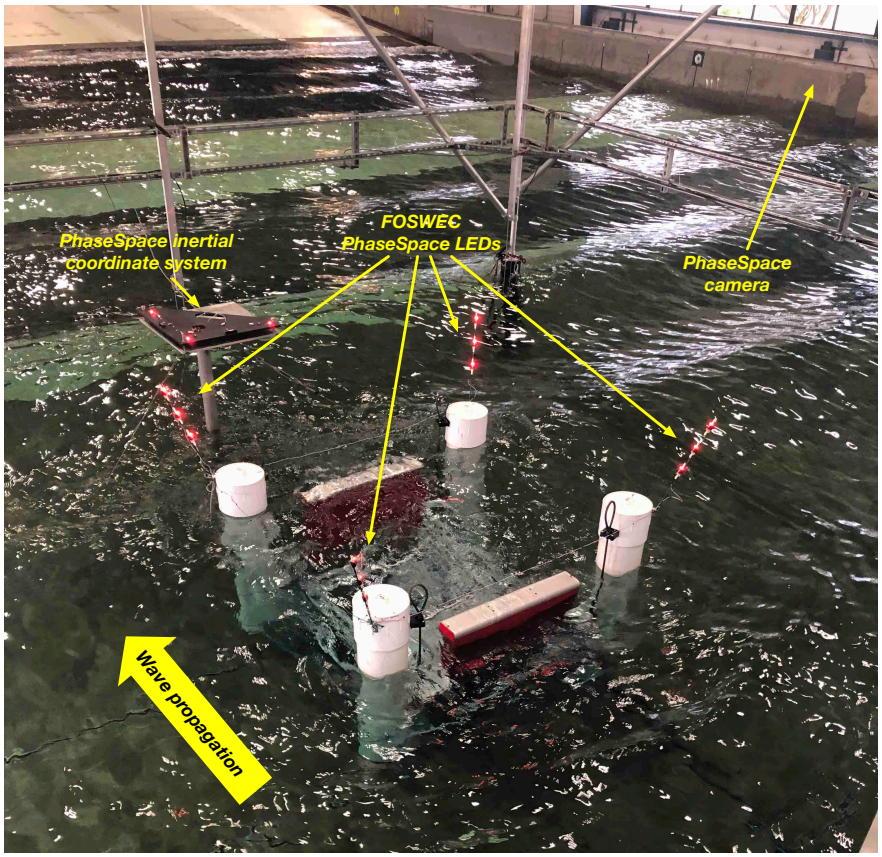

Figure 2-10 PhaseSpace components.

- Finally, the y-axis is the alongshore coordinate (parallel to the wavemaker piston). The y-axis origin ($y = 0$) is at the alongshore centerline of the tank, i.e., halfway between two vertical planes that best fit the tank walls. The y-axis is measured in meters and positive to the left when facing onshore, so that the coordinate system is right-handed.

In the DWB, x is positive west and y is positive south.

PhaseSpace coordinates $(x_{ps}, y_{ps}, z_{ps})$are defined differently from HWRL coordinates. PhaseSpace data is collected with an origin $(x_{ps}, y_{ps}, z_{ps}) = (0, 0, 0)$ at the origin LED of the PhaseSpace coordinate axis definition square. It measures distance in millimeters and attitude of each rigid body (body rotations applied in the order yaw then pitch then roll) in radians. x_{ps} is positive onshore, y_{ps} is positive upwards, and z_{ps} is positive to the right when facing onshore (away from the wavemaker paddle), so that the coordinate system is right-handed.

For the SandiaFOSWEC project, x_{ps} is positive west and z_{ps} is positive north. Therefore x_{ps} is positive in the same direction as x, y_{ps} is positive in the same direction as z, but z_{ps} is positive in the opposite direction from y.

2.2. Basin layout & assembly

The DWB measures 48.8 m (160 ft) long by 2.1 m (7 ft) deep by 26.5 m (87 ft) wide, and has a maximum water depth of 1.5 m (5 ft). The DWB is equipped with 29-segmented piston-type waveboards capable of generating either periodic or random directional waves to simulate the wave spectra associated with large storms. Detailed information on the DWB and HWRL available instrumentation can be found in the HWRL web site. The DWB shall be set up with a 1:10 steel beach at the onshore end for wave dissipation.

Figure 2-11 shows a diagram of the FOSWEC v2 layout with the DWB. This diagram shows the FOSWEC v2 along with the basin wave probes used in the previous WEC-Sim FOSWEC v1 test. Additionally, the mooring lines and mooring anchor points are shown. Figure 2-12 shows the planned layout of wave probes within the basin. Probes 1-4 are self calibrating gauges, 5-14 are cantilever gauges, and uswg1-4 are ultrasonic gauges. The scaffolding frame used to mount wave gauges in the proximity of the FOSWEC v2 is shown in Figure 2-13.

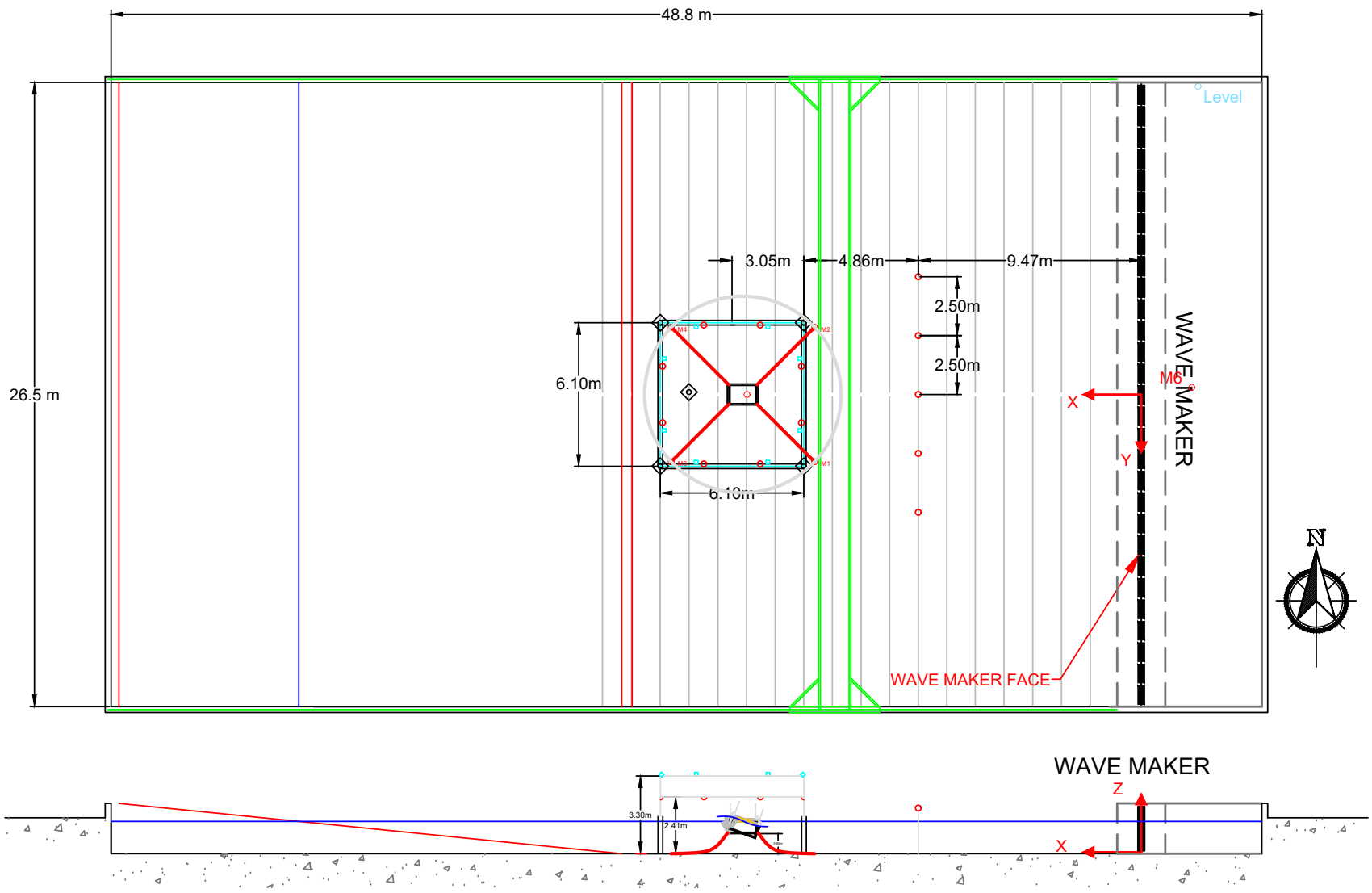

Figure 2-11 Layout of HRWL basin with FOSWEC v2 and wave probes.

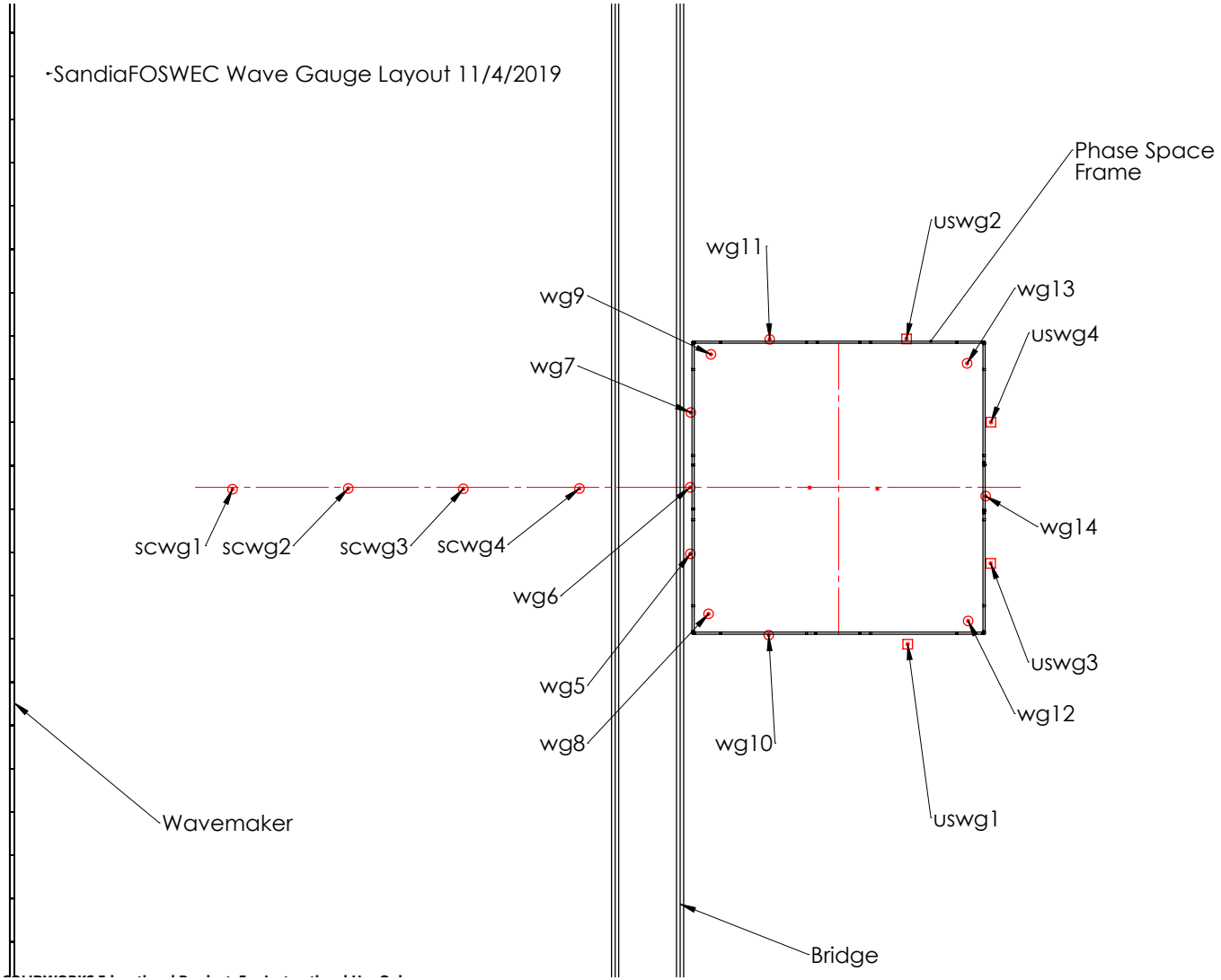

Figure 2-12 Layout of wave probes (scwg: self-calibrating wave gauge; uswg: ultra sonic wave gauge; wg: cantilever wave gauge).

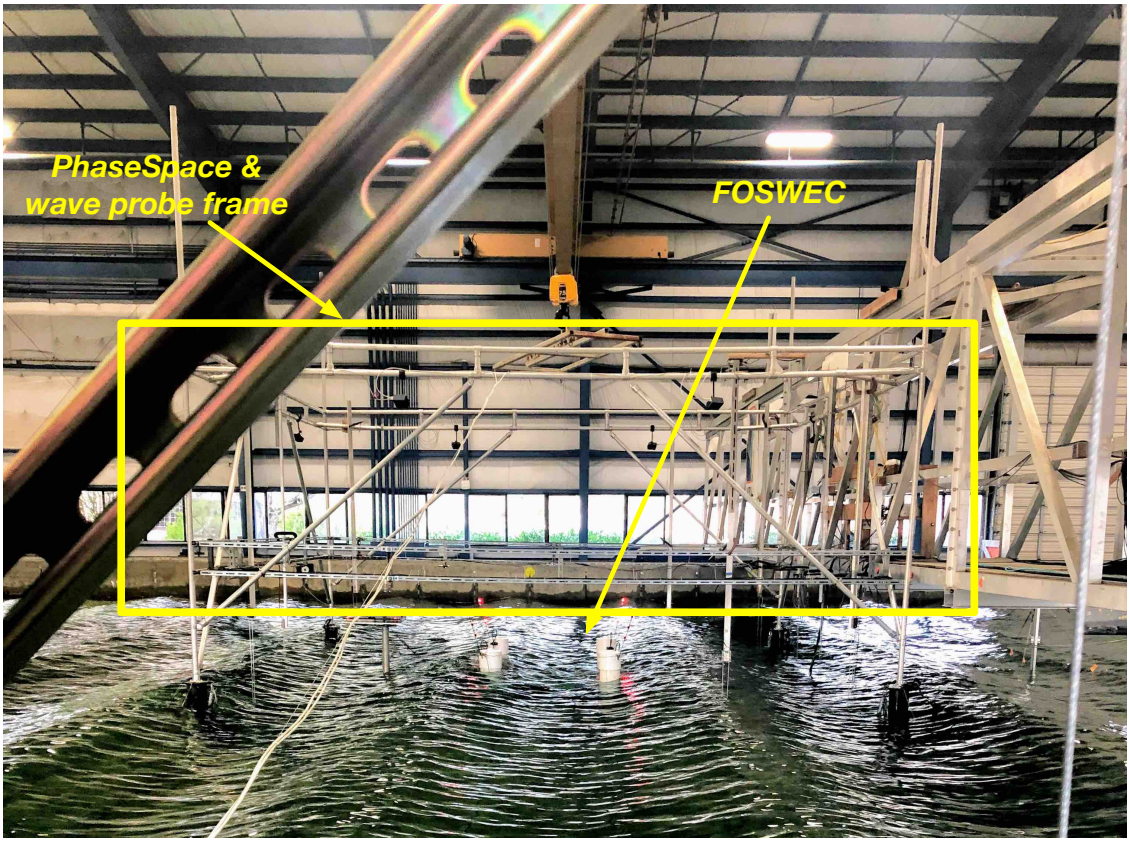

Figure 2-13 PhaseSpace camera & wave probe frame.

2.3. Wave cases

The following wave types were considered during this test:

- **Regular waves** - Waves with a single frequency component
- **Irregular idealized spectra** - Ocean waves were approximated by JONSWAP spectra run in two modes
  - **Non-repeating** - In this case, the number of frequency components were chosen such that no repeat of the wave sequence is observed during the experiment. The repeat period of the wave train defined by evenly spaced frequency components is

$$T_r = \frac{2\pi}{\Delta\omega} \tag{1}$$

    Here, $\Delta\omega$ is the frequency spacing in rad/s. For a non-repeating sequence, $\Delta\omega$ can be set such that $T_r > T_{\text{test}}$, where T_{test} is the test length.
  - **Repeating** - In this case, the number of frequency components is limited such that the wave sequence repeats multiple times within a single experiment ($T_r < T_{\text{test}}$).
- **Chirps** - Waves in which the wave frequency, $f(t)$, changes with respect to time following

$$f(t) = f_0 + \beta t, \tag{2}$$

  where β is the rate change of the frequency and f_0 is the starting frequency.
- **Pink multisines** - Pseudo-randomly phased waves comprised of i evenly-spaced frequency components where component amplitude a is inversely proportional to frequency.

$$a_i \propto \frac{1}{f_i} \tag{3}$$

Figure 2-14 shows a plot of the JONSWAP and regular wave cases considered using the nondimensional regime axes suggested by [7]. Note that these waves are labeled using the convention of this report (Tables 2-2, 2-3, 2-4, and 2-5 [2] [3].). From Figure 2-14, we can see that the majority of the waves are in the intermediate depth regime. Roughly half of the waves are well represented by linear theory. Additionally, we can see from Figure 2-14 that breaking is possible or likely, especially in the case of irregular waves for which the plot refers to the significant wave height, in the "D" and "E" class waves.

[2] Irregular waves were used with γ values of both 1 and 3.3. The Irregular Wave ID code tabulated uses # as a placeholder for either value, e.g. J1A-g3.3 implies a JONSWAP wave with a 0.015 m mean wave height and a 0.19 Hz peak frequency with $\gamma = 3.3$.

[3] Pink waves with 3 distinct phase realizations were used. Pink Wave ID code tabulated uses # as a placeholder to distinguish these phase realizations

Table 2-2 Regular Wave ID Matrix

Freq. (Hz)	Wave Height (m)				
-	0.015	0.045	0.136	0.250	0.40
0.19	R1A	R1B	R1C	R1D	R1E
0.26	R2A	R2B	R2C	R2D	R2E
0.38	R3A	R3B	R3C	R3D	R3E
0.51	R4A	R4B	R4C	R4D	R4E
0.64	R5A	R5B	R5C	R5D	R5E
0.80	R6A	R6B	R6C	R6D	R6E

Table 2-3 Irregular Wave ID Matrix

Peak Freq. (Hz)	Mean Wave Height (m)				
-	0.015	0.045	0.136	0.250	0.40
0.19	J1A-g#	J1B-g#	J1C-g#	J1D-g#	J1E-g#
0.26	J2A-g#	J2B-g#	J2C-g#	J2D-g#	J2E-g#
0.38	J3A-g#	J3B-g#	J3C-g#	J3D-g#	J3E-g#
0.51	J4A-g#	J4B-g#	J4C-g#	J4D-g#	J4E-g#
0.64	J5A-g#	J5B-g#	J5C-g#	J5D-g#	J5E-g#
0.80	J6A-g#	J6B-g#	J6C-g#	J6D-g#	J6E-g#

Table 2-4 Chirp Wave ID Matrix

Freq. Range (Hz)	Mean Wave Height (m)				
-	0.015	0.045	0.136	0.250	0.40
0.05 to 1.5	ChirpA	ChirpB	ChirpC	ChirpD	ChirpE

Table 2-5 Pink Wave ID Matrix

Freq. Range (Hz)	Mean Wave Height (m)				
-	0.015	0.045	0.136	0.250	0.40
0.05 to 1.5	Pink#A	Pink#B	Pink#C	Pink#D	Pink#E

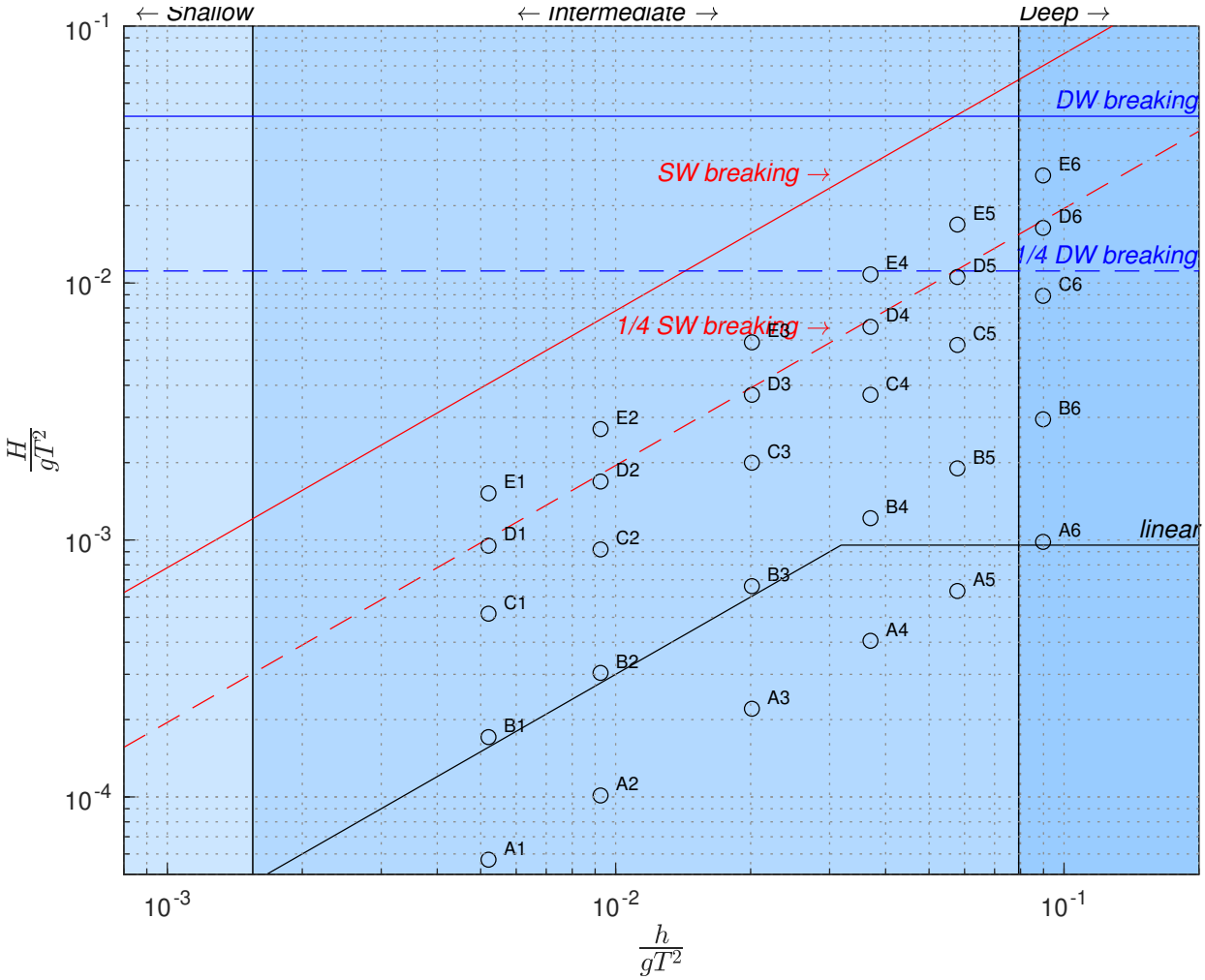

Figure 2-14 Wave regimes based on wave height and peak period using the nondimensional regime axes suggested by [7].

3. RESULTS

The results of this testing campaign are summarized in the two subsequent sections. First, the results of system identification (SID) tests are provided in Section 3.1. Next, using the models produced via SID, closed loop control tests were executed. These results are summarized in Section 3.2.

3.1. System identification

The SID methods applied in this experiment follow the procedures suggested in [2]. These methods are based on the broader engineering practices of SID applied in many fields, including aerospace, automotive, and electronic engineering (see, e.g., [12, 8]). These methods rely on the application of broadband repeating signals to excite the system under consideration. As mentioned in Section 1, a key goal of this test is to determine whether these methods can readily be applied a broad range of devices.

Two types of tests were conducted to identify reduced order numerical models of the FOSWEC v2 dynamics. Figure 3-1 shows the work-flow for this system identification process. The target model structure is shown in grey on the right side of Figure 3-1. The two component models, the excitation model denoted by H and the impedance model denoted by Z_i, were obtained through two respective tests.

First, as shown in the upper half of Figure 3-1, the impedance model was obtained via force oscillation (a.k.a., "radiation") tests. In these tests, no waves were produced by the wave maker. A series of band-limited white noise signals, with different random phasings, were sent to the bow and aft flap motors. A minimum of two tests of this type are required to identify the two-input, two-output impedance system for the FOSWEC v2.

The resulting 2×2 admittance model ($Y = \frac{1}{Z_i}$) relating flap torque (input) to flap velocity (output) is shown in Figure 3-2. Both nonparametric (red) and parametric (blue) admittances are shown in Figure 3-2. The parametric models are fifth-order transfer functions.

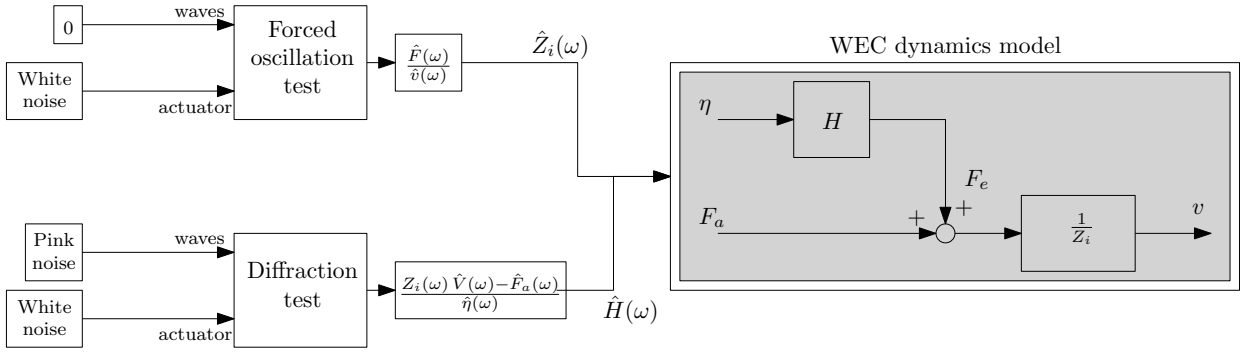

Figure 3-1 System identification workflow used for FOSWEC v2 (adapted from [1]).

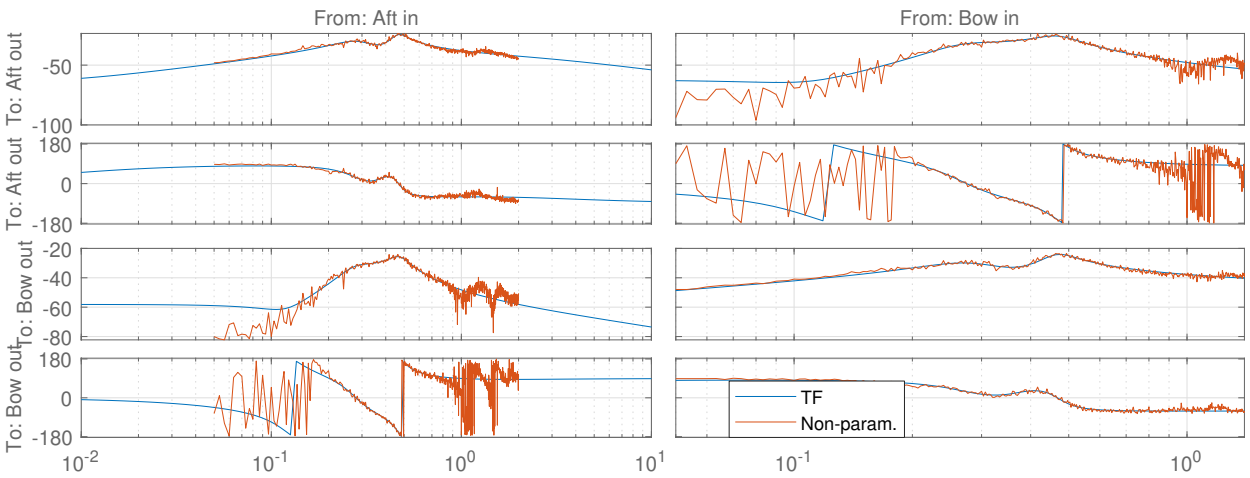

Figure 3-2 FOSWEC v2 admittance (input: torque, output: velocity) Bode plot (in Hz and dB) showing nonparametric and parametric ("TF") models.

In addition to examining the admittance in Figure 3-2, it is useful to review the resulting control parameters. If we consider a proportional derivative (PD) controller operating on position, we can find the following controller gains based on the device impedance.

$$\begin{aligned} \text{Spring term: } K_p &= \omega \Im\{Z_i^*\} \\ \text{Damping term: } K_d &= \Re\{Z_i^*\} \end{aligned} \tag{4}$$

These control gains are plotted in Figure 3-3. The so-called "diagonal terms," which represent each flap's effect on itself, are plotted in blue (both the aft and bow flap results are shown together as they are so similar). The off-diagonal or "cross-coupling" terms are shown in red.

With a satisfactory impedance model in hand, excitation tests, as depicted in the lower half of Figure 3-1, were conducted. Pink waves were sent by the wave maker. As suggested by [2], the excitation tests were conducted without locking the device Instead, the impedance model was used to "subtract" the effect of the uncorrelated band-limited white-noise signals simultaneously sent to the flap actuators. These models were obtained using the data from experiments 171-175 (Appendix C).

$$H(\omega) = \frac{Z_i(\omega)\hat{V}(\omega) - \hat{F}_a(\omega)}{\hat{\eta}(\omega)}. \tag{5}$$

Figure 3-4 shows two excitation models each for the bow and aft flaps: an averaged model that uses the data from each of the five experiments and a smoothed model that uses a windowing method (MATLAB function: `spa`).

From Figure 3-4, we can see that the excitation on the flaps is fairly constant for $f < 0.6$ Hz. Note however that some of the dips shown in the excitation averaged models (non-smoothed) manifest significantly in the physical system: during chirp tests, the flaps were seen to have very little excitation at specific frequencies.

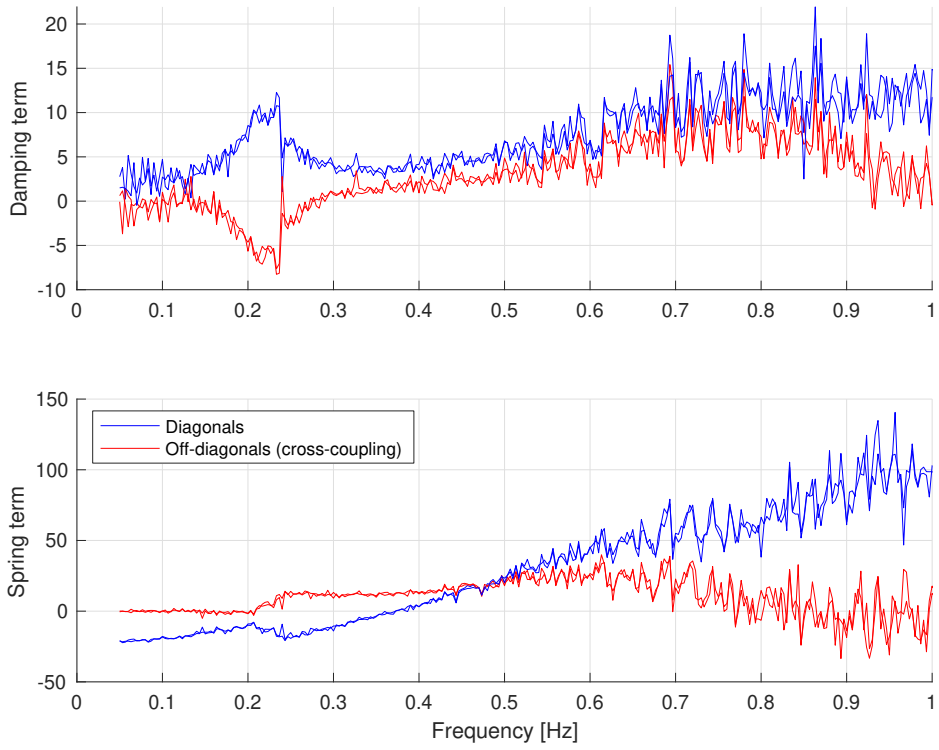

Figure 3-3 FOSWEC v2 feedback control terms.

3.1.1. Drivetrain response

The dynamic response of the drivetrain is useful for control design purposes, particular to study stability margins and sensitivity of response to noisy signal. The response is obtained by forcing the FOSWEC, while in the water, with white noise signals for the commanded current on both the aft motor (I_a) and the bow motor (I_b); the power spectral density of the input signals is shown in Figure 3-5. The white noise signals are generated using different seeds and they are sent simultaneously to both aft and bow drives; the data of this experiment is collected in the test with ID 226 (see Appendix C).

The measured outputs are the angular velocity of the motors shaft (w_{a_m} for aft motor; w_{b_m} for bow motor) and the angular velocity of the flaps (w_{a_f} for aft flap; w_{b_f} for bow flap). Figure 3-6 shows the Bode plot obtained by using the Matlab function for spectral analysis `spa`[4], where G_m^m is the response between the commanded currentS and the angular velocity of the rotors, and G_m^f is the response between the commanded currents and the angular velocity of the flaps; these response functions are defined as:

$$\begin{bmatrix} w_{a_m} \\ w_{b_m} \end{bmatrix} = G_m^m \begin{bmatrix} I_a \\ I_b \end{bmatrix} \qquad \begin{bmatrix} w_{a_f} \\ w_{b_f} \end{bmatrix} = G_m^f \begin{bmatrix} I_a \\ I_b \end{bmatrix} \tag{6}$$

Figure 3-6 shows that the drivetrains of both flaps have almost identical response, and that the interaction between the two flaps occurs mostly at low frequency (<1Hz) and it's due to the hy-

[4]https://www.mathworks.com/help/ident/ref/spa.html

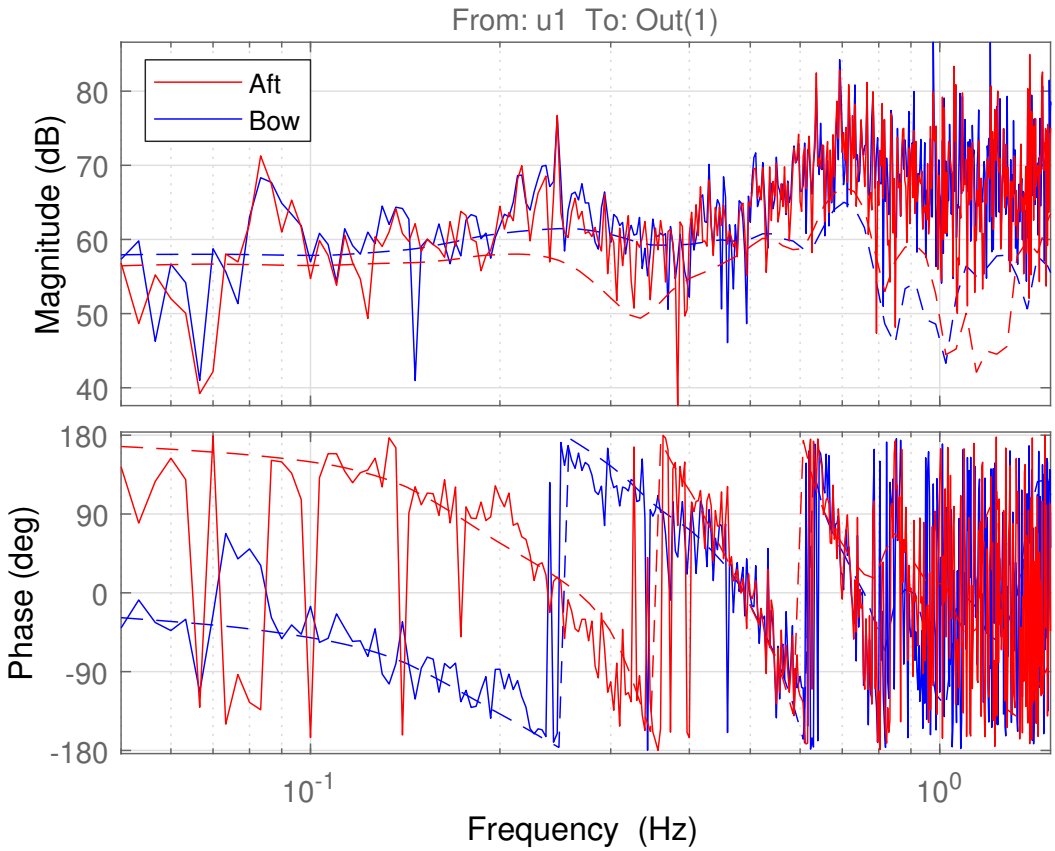

Figure 3-4 FOSWEC v2 excitation (input: wave probe, output: excitation torque) Bode plot showing averaged and smoothed models.

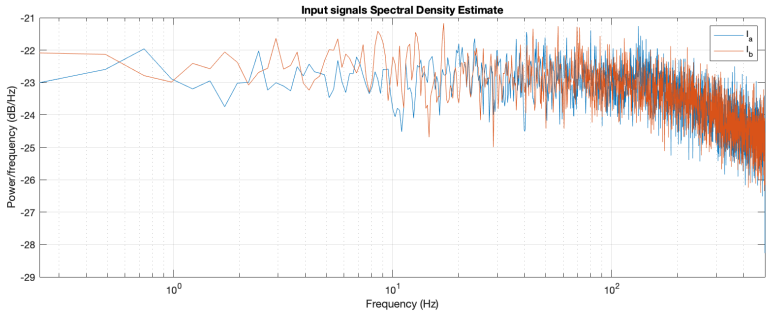

Figure 3-5 Spectral density estimates of the current command signals

drodynamic coupling. At higher frequency, the off-diagonal terms are significantly smaller than the diagonal terms.

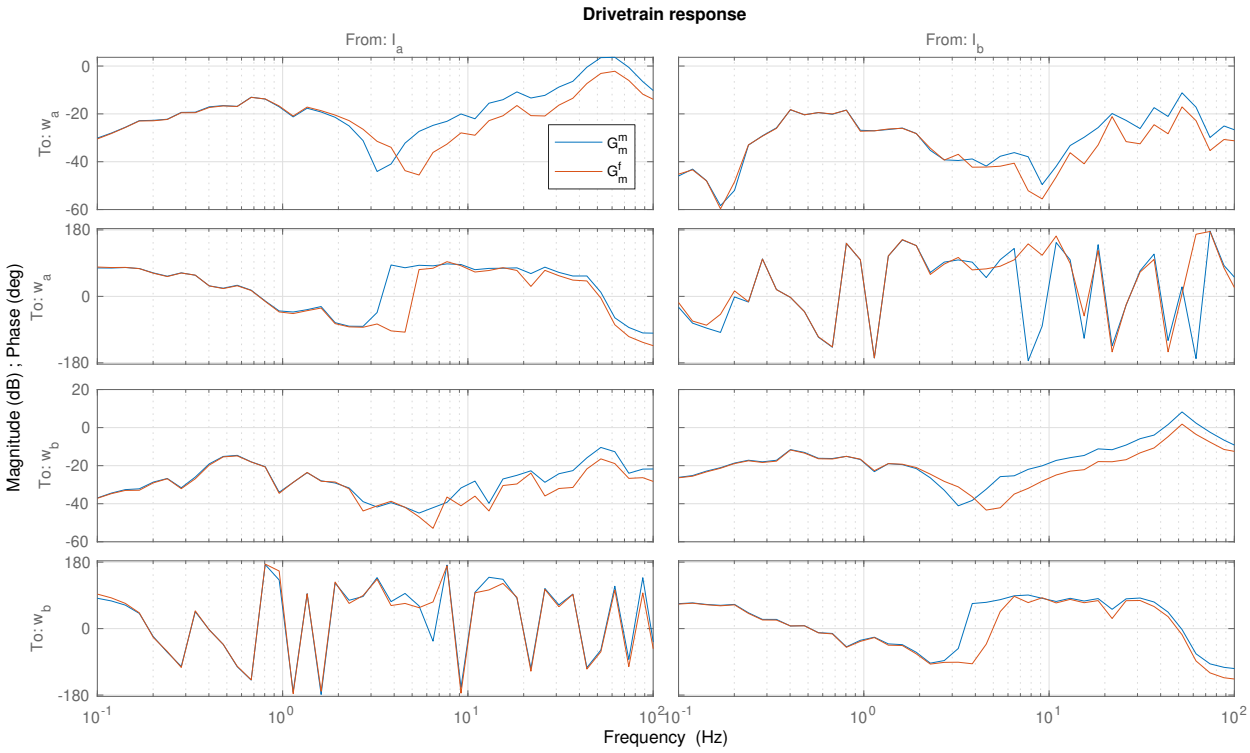

Figure 3-6 Bode diagram of the drivetrain responses

3.2. Closed loop control

Based on the models produced in Section 3.1, a set of closed loop control tests were conducted in both regular and irregular waves.

Figure 3-7 shows the control performance results in irregular J1C-g3.3 waves (test 229). As previously discussed in [3], a single test with a short repeat period was used to evaluate control performance across a set of gain tunings. Using a diagonal controller of the form

$$F_a = (K_p^{j,j} + i\omega K_d^{j,j})X(\omega) \tag{7}$$

where j is the index of the flap (1 for bow, 2 for aft) and X is the angular position of each flap. The four controller parameters were varied over a prescribed range using a latin hypercube method every 180 s, the repeat period of the incident waves. This creates a 4-D grid over which power capture wave evaluated for each gain combination. Mechanical power calculated at the motor shaft is

$$P_m = \omega_a(K_t I_a) + \omega_b(K_t I_b) \tag{8}$$

where ω_a and ω_b are the angular velocity (rad/s) of the aft and bow flap, respectively, K_t is the motor constant (N-m/A), and I is the current in the motor driving the aft and bow flaps (similarly

denoted by the subscripts). This is averaged in time over the wave repeat period to produce the plotted quantities. Dissipated electrical power can be similarly calculated as

$$P_{dis} = \frac{3}{2} R_{pn}(I_a^2 + I_b^2) \tag{9}$$

where R_{pn} is the phase-to-neutral resistance of the three-phase motor. This value is similarly averaged. Finally, total absorbed electrical power is calculated

$$P_{abs} = K_t(I_a\omega_a + I_b\omega_b) + P_{dis} \tag{10}$$

noting the sign convention. This is similarly averaged and includes captured and dissipated electrical powers.

The upper most plot in Figure 3-7 shows the mechanical absorbed power, the middle plot shows the dissipated electrical power, and the lower shows the absorbed electrical power. Comparing results at common sets of gain values (x-axis) across the rows of the sub-plot, control parameters that maximized the mechanical power absorption tend to decrease the electrical power absorbed, and vice versa. This implies that optimization of electrical power occurs at a different set of conditions than mechanical power due to the dynamics of the power conversion system, and thus presents a distinct control design problem. This is consistent with [3]. Note that due to the drive train design of the FOSWEC v2, which is targeted towards torque tracking, not energy generation, all of the gain combinations result in net negative generated electrical power.

To understand the response surface of the FOSWEC v2 power capture, a series of three two-dimensional contours can be considered, each a two-dimensional "slice" of the four-dimensional surface defined by the controller gains. Figure 3-8 shows a contour of mechanical energy absorption a range of symmetric controller tunings (i.e., $K^{(1,1)} = K^{(2,2)}$). In this case, we can see that mechanical power increases for larger negative values of the spring constant (K_p). A negative spring constant implies that the controller was attempting to counteract the positive hydrostatic stiffness spring term. This reduction in total stiffness would decrease the resonant frequency of the WEC. Figure 3-2 indicates that a natural system resonance (a peak of admittance) occurs at ~ 0.4 Hz, while the peak frequency of the exciting wave is 0.19 Hz (Table 2-3). This is thus an intuitive result: power capture is increasing as the controller brings the WEC into resonance with the exciting wave. Note particularly that this agrees with the relationship predicted by Figure 3-3: the diagonal spring term is negative until frequency > 0.4 Hz, at which point it changes sign.

Additional contours can be obtained by setting the either the damping (k_d) or spring (k_p) terms fixed. These contours are shown in Figure 3-9 and Figure 3-10 for the spring and damping terms, respectively. At this sea-state, both contours suggest that higher absolute values of K_d and K_p would likely allow increased mechanical power capture, but were outside of the evaluated range. Elevating these gains further was found to cause system instability likely due to the amplification of sensor noise. This emphasizes the importance of carefully designing the PTO system and sensors in conjunction with control laws to affect control parameters allowing optimal energy capture.

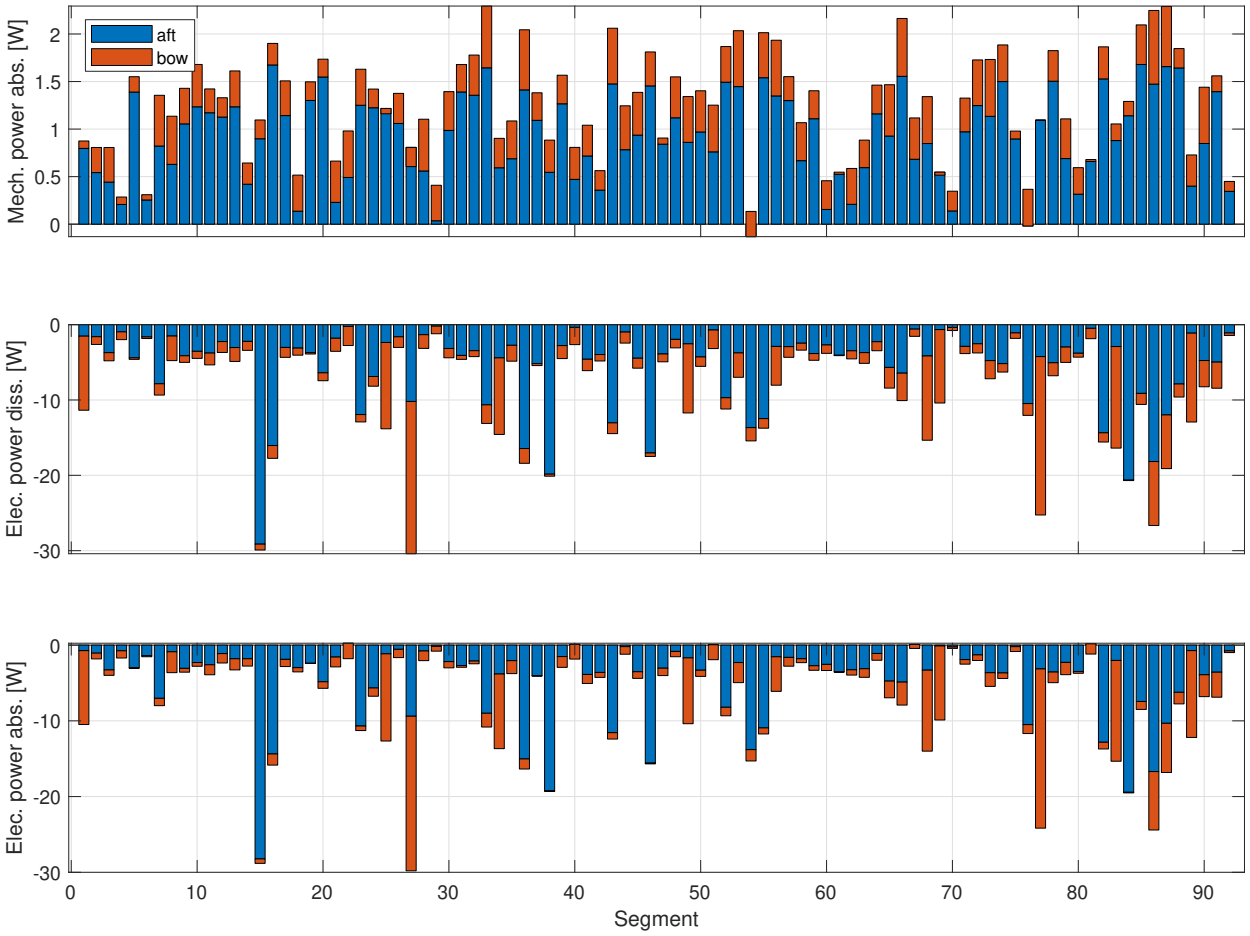

Figure 3-7 Irregular control performance from irregular J1C-g3.3 (test 229) showing individual gain segments .

Consistent trends can be observed from contrasting sea states, as well. Figure 3-11 through Figure 3-14 show analogous results from sea-state R4C, a regular wave with an excitation frequency slightly greater than device natural frequency (Table 2-2). As expected from Figure 3-3, $K_p > 0$ for maximum power producing cases. Although the power surface remains convex over the tested values, it is more featured than the corresponding irregular wave surfaces, perhaps demonstrating the coupling effects of the out-of-phase flap responses observed at this frequency (Figure 3-2). Despite the more complex power surface, gains exhibiting high mechanical power capture do not maximize electrical power capture, and vice versa. However, in this case of a regular wave near the resonant device frequency, some gain combinations do generate a small amount of electrical power Figure 3-11). Again, the tested range of gains do not bound the mechanical power optimum: larger amplitude gains are desirable but not attainable on device hardware.

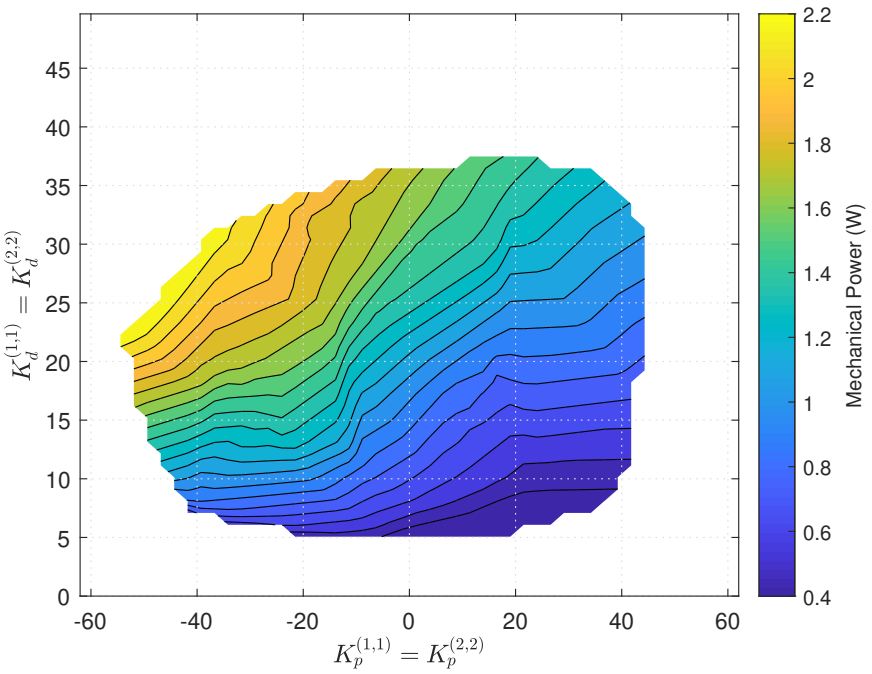

Figure 3-8 Irregular control performance from J1C-g3.3 (test 229) with symmetric gain tunings.

4. CONCLUSION

This test report presents a sampling of results from testing of the FOSWEC v2. A concise set of tests were performed to obtain an empirical model for the device impedance and wave excitation. Based on this impedance model, a set of causal impedance matching controls were designed and shown to perform as expected within the limitations of device hardware.

These findings confirm that the engineering methods and workflows originally developed and implemented for the WaveBot can perform well on a wide range of wave energy device archetypes. Consistent with WaveBot testing, the FOSWEC v2 device showed a substantial distinction between optimal control for electrical power capture and optimal control for mechanical power capture. This reiterates the importance of cooperative design of the controller, WEC, and PTO system, as their coupled dynamics and capabilities must be well-suited to each other to attain optimal electrical power capture.

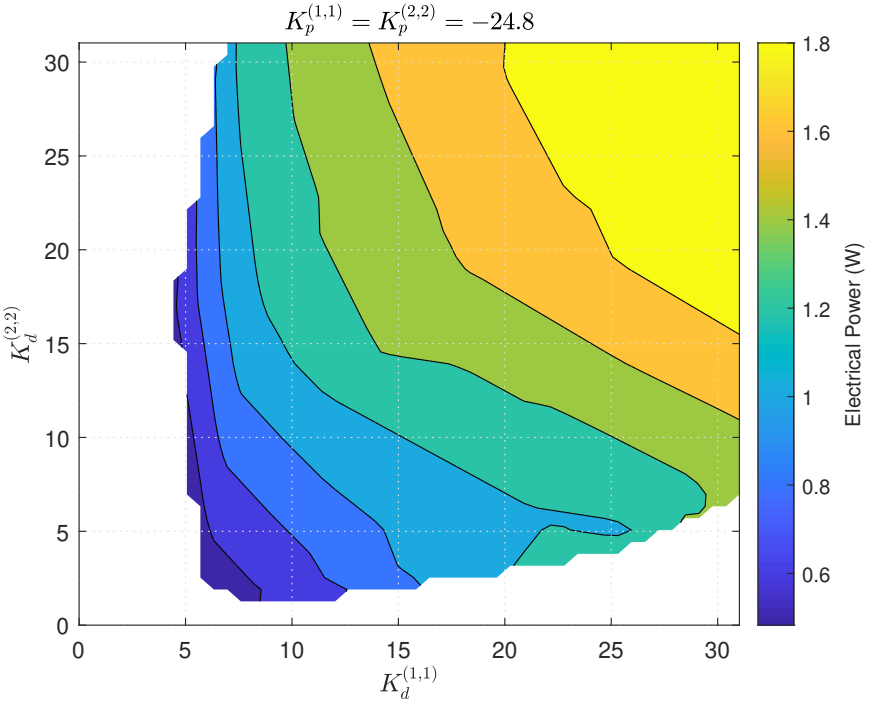

Figure 3-9 Irregular control performance from J1C-g3.3 (test 229) with constant spring terms ($k_p = -2$).

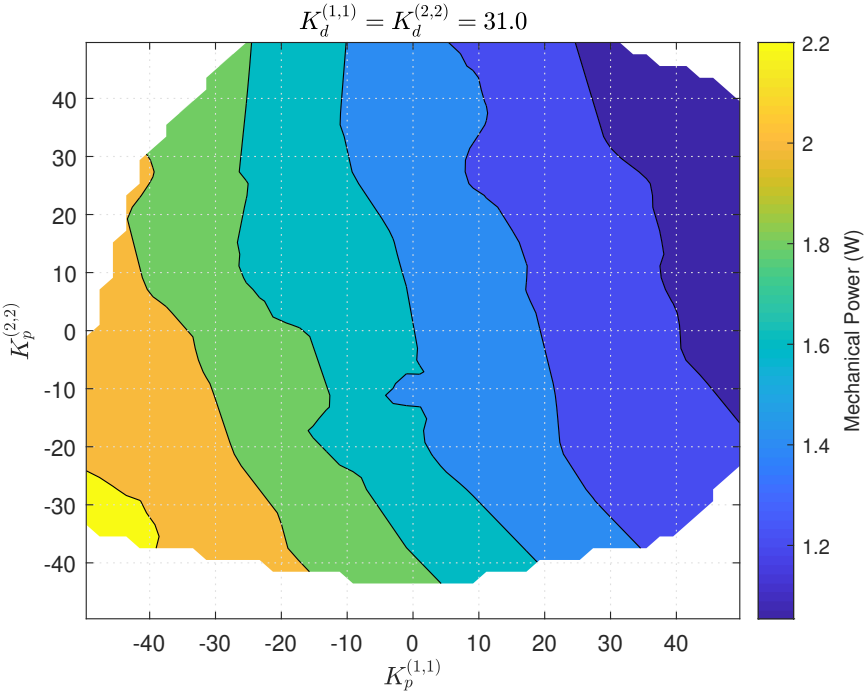

Figure 3-10 Irregular control performance from J1C-g3.3 (test 229) with constant damping terms ($k_d = 2.5$).

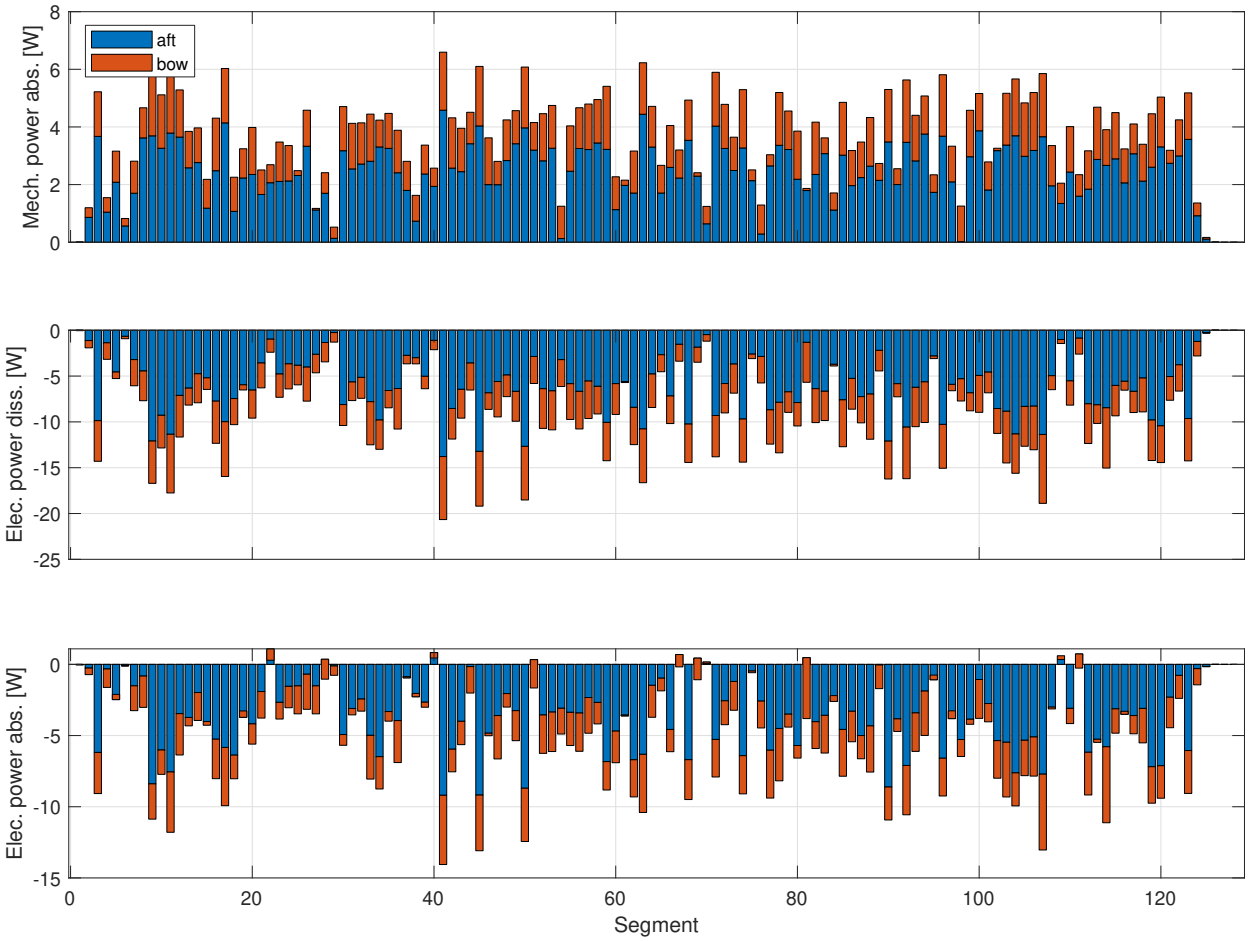

Figure 3-11 Regular control performance from R4C (test 228) showing individual gain segments.

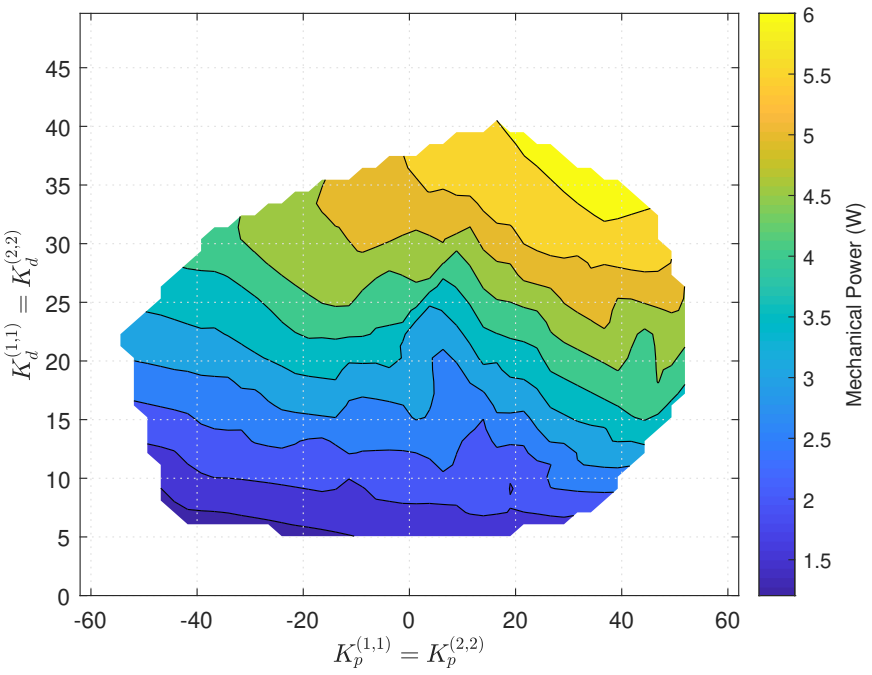

Figure 3-12 Regular control performance from R4C (test 228) with symmetric gain tunings.

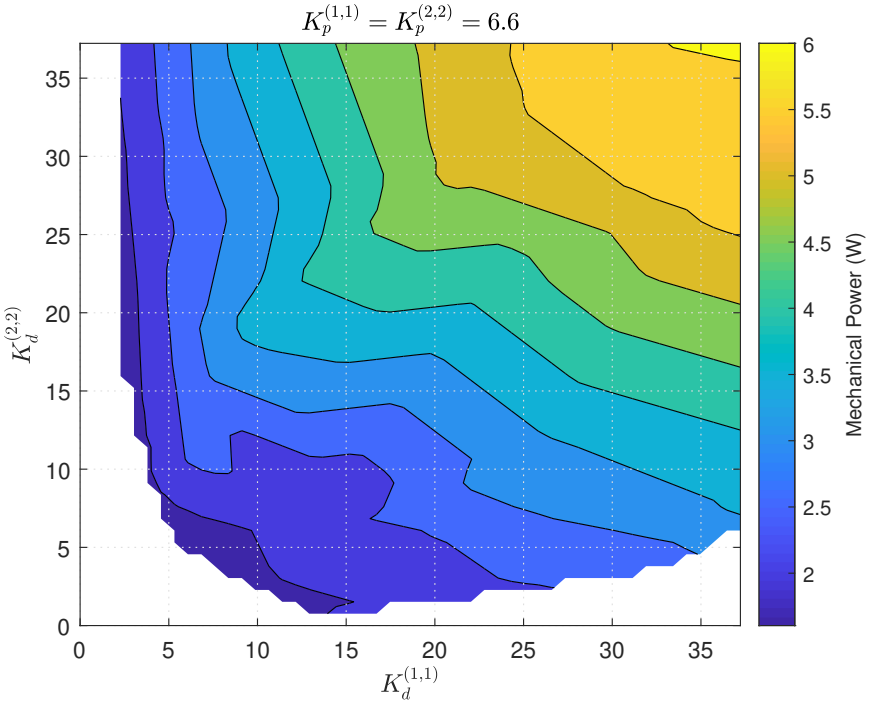

Figure 3-13 Regular control performance from R4C (test 228) with constant spring terms ($k_p = 2$).

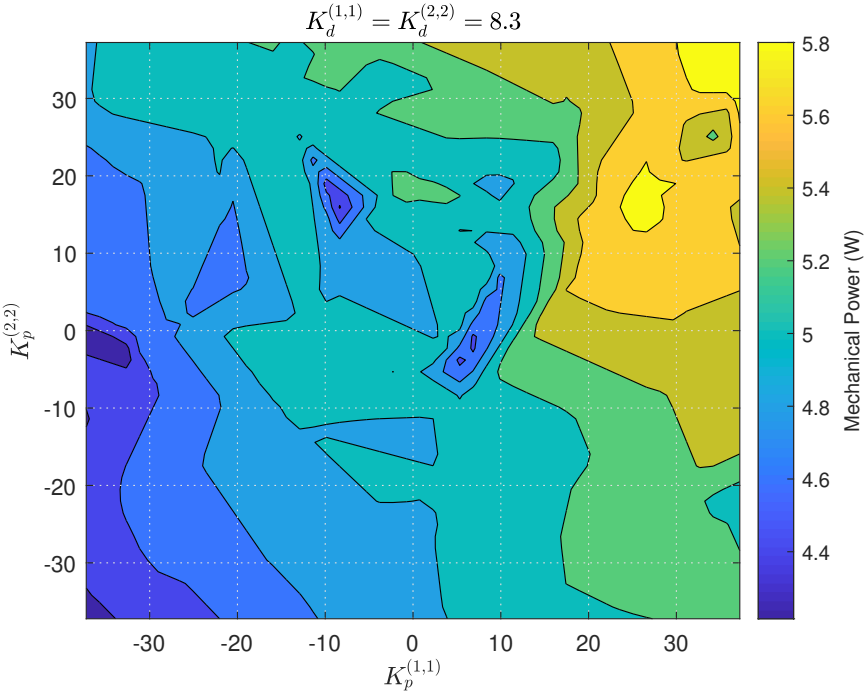

Figure 3-14 Regular control performance from R4C (test 228) with constant damping terms ($k_d = 2.5$).

REFERENCES

[1] Giorgio Bacelli and Ryan G. Coe. WEC system identification and model validation. In *Marine Energy Technology Symposium (METS2017)*, Washington, D.C., 2017.

[2] Giorgio Bacelli, Ryan G. Coe, David Patterson, and David Wilson. System identification of a heaving point absorber: Design of experiment and device modeling. *Energies*, 10(10):472, 2017.

[3] Giorgio Bacelli, Steven J. Spencer, David C. Patterson, and Ryan G. Coe. Wave tank and bench-top control testing of a wave energy converter. *Applied Ocean Research*, 86:351 – 366, 2019.

[4] Bret Bosma, Asher Simmons, Pedro Lomonaco, Kelley Ruehl, and Budi Gunawan. Wec-sim phase 1 validation testing: Experimental setup and initial results. In *ASME 2016 35th International Conference on Ocean, Offshore and Arctic Engineering*, pages V006T09A025–V006T09A025. American Society of Mechanical Engineers, 2016.

[5] Ryan G. Coe, Giorgio Bacelli, David Patterson, and David G. Wilson. Advanced WEC Dynamics & Controls FY16 testing report. Technical Report SAND2016-10094, Sandia National Labs, Albuquerque, NM, October 2016.

[6] Ryan G. Coe, Giorgio Bacelli, Steven J. Spencer, and Hancheol Cho. Initial results from wave tank test of closed-loop WEC control. Technical Report SAND2018-12858, Sandia National Laboratories, Albuquerque, NM, 2018.

[7] Bernard Le Mehaute. *An introduction to hydrodynamics and water waves*. Springer-Verlag, New York, 1976.

[8] R. Pintelon. Frequency-domain subspace system identification using non-parametric noise models. *Automatica*, 38(8):1295 – 1311, 2002.

[9] Kelley Ruehl, Dominic Forbush, Pedro Lomonaco, Bret Bosma, Asher Simmons, Budi Gunawan, Giorgio Bacelli, and Carlos Michelen. Experimental testing of a floating oscillating surge wave energy converter. Technical Report SAND2019-3087, Sandia National Laboratories, 2019.

[10] Kelley Ruehl, Dominic D Forbush, Yi-Hsiang Yu, and Nathan Tom. Experimental and numerical comparisons of a dual-flap floating oscillating surge wave energy converter in regular waves. *Ocean Engineering*, 196:106575, 2020.

[11] Kelley Ruehl, Carlos Michelen, Bret Bosma, and Yi-Hsiang Yu. WEC-Sim phase 1 validation testing: Numerical modeling of experiments. In *ASME 2016 35th International Conference on Ocean, Offshore and Arctic Engineering*, pages V006T09A026–V006T09A026. American Society of Mechanical Engineers, 2016.

[12] J. Schoukens, G. Vandersteen, K. Barbé, and R. Pintelon. Nonparametric preprocessing in system identification: A powerful tool. In *2009 European Control Conference (ECC)*, pages 1–14, Aug 2009.

APPENDIX A. DATA STRUCTURE

Raw data from the FOSWEC v2 EtherCAT network was logged at either 100 Hz, 1 KHz, or 10 KHz by the real-time computer into `*.dat` files. The variable-rate logging was intended to reduce file size without degrading data quality by logging semi-static or more slowly varying operating parameters at a reduced rate. The rate at which raw data is logged is indicated in the following list. This raw data collected by the FOSWEC v2 EtherCAT network was processed and saved in a consistent format as a `data.mat` file data structure. To facilitate plotting and further processing, all time-series in `data.mat` have been re-sampled to 1 KHz.

- `data.aft`: This field contains data from the aft flap and drive-train
  - `I_m`: the measured current (A) at the motor drives.
  - `I_abs`: the controller-commanded current (A), including I_ref, sent to the motor drives from Simulink (10 KHz).
  - `I_ref`: the open-loop component current (A) (10 KHz).
  - `V_DC`: the DC bus voltage at the motor drive (10 KHz).
  - `w_m`: motor shaft velocity (rad/s) as measured by the motor encoder (1 KHz).
  - `w_f`: flap shaft velocity (rad/s) calculated from the motor encoder $w_f = w_m/N$ (1 KHz).
  - `th_m`: motor shaft position (rad) as measured by the motor encoder (1 KHz).
  - `th_f`: flap shaft position (rad) as calculated from the motor encoder $th_f = th_m/N$ (1 KHz).
  - `ssi_m`: motor position (rad) as calculated from the flap encoder $ssi_m = Nssi_f$ (1 KHz).
  - `ssi_f`: flap shaft position (rad) as measured from the flap encoder (1 KHz).
  - `ATI_Fx`: the force (N) on the flap load cell in the wave propagation direction (1 KHz).
  - `ATI_Fy`: the force (N) on the flap load cell in the along-wave direction (1 KHz).
  - `ATI_Fz`: the force (N) on the flap load cell in the vertical direction (1 KHz).
  - `ATI_Tx`: the torque (N-m) on the flap load cell about the shaft (1 KHz).
  - `ATI_Ty`: the torque (N-m) on the flap load cell about the horizontal perpendicular to the shaft (1 KHz).
  - `ATI_Tz`: the torque (N-m) on the flap load cell about the vertical perpendicular to the shaft (1 KHz).
  - `temp_res`: the resistance (Ohms) of the motor thermistor (100 Hz).
  - `temp`: the temperature (C) calculated from the resistance of the motor thermistor (100 Hz).
  - `temp_stat`: unused.

  - `KP_auto`: the k_p control gain suggested by the auto-tuner block (unused if autotuner is not enabled) (100 Hz).
  - `KD_auto`: the k_d control gain suggested by the auto-tuner block (unused if autotuner is not enabled) (100 Hz).
  - `CCKP_auto`: the off-diagonal k_p control gain suggested by the auto-tuner block (unused if autotuner is not enabled) (100 Hz).
  - `CCKD_auto`: the off-diagonal k_d control gain suggested by the auto-tuner block (unused if autotuner is not enabled) (100 Hz).
  - `KP_used`: the k_p control gain used by the controller. Note that controller must be enabled for commands to be passed to motor (100 Hz).
  - `KD_used`: the k_d control gain used by the controller. Note that controller must be enabled for commands to be passed to motor (100 Hz).
  - `CCKP_used`: the off-diagonal k_p control gain used by the controller. Note that controller must be enabled for commands to be passed to motor (100 Hz).
  - `CCKD_used`: the off-diagonal k_d control gain used by the controller. Note that controller must be enabled for commands to be passed to motor (100 Hz).
  - `AftMode`: the operating mode of the motor driver. Should be a constant (100 Hz).
  - `t`: timestamp associated with the 1 KHz data.
  - `N`: FOSWEC v2 gear ratio from Table 2-1.
  - `Kb_pp_peak`: motor nameplate maximum phase-to-phase back-EMF (V-s/rad).
  - `R_pp`: motor nameplate phase-to-phase resistance (Ohm).
  - `R_pn`: motor nameplate phase-to-neutral resistance (Ohm).
  - `Kt`: motor nameplate torque constant (N-m/A).
  - `Kb`: motor nameplate back-EMF constant (V-s/rad).
- `data.bow`: This field contains data from the bow flap and drive-train. The subfields are identical to data.aft, except subfields containing "aft" have been replaced to instead contain "bow."
- `data.hull`: This field contains data and diagnostics from hull-based sensors.
  - `H_P1`: the external hull pressure (Pa) as measured by relative pressure transducer 1 (1 KHz).
  - `H_P2`: the external hull pressure (Pa) as measured by relative pressure transducer 2 (1 KHz).
  - `H_P3`: the external hull pressure (Pa) as measured by relative pressure transducer 3 (1 KHz).

- `H_P4`: the external hull pressure (Pa) as measured by relative pressure transducer 4 (1 KHz).
- `H_Pabs`: the internal hull pressure (Pa) as measured by the absolute pressure sensor (1 KHz).
- `Leak`: a binary (0 no, 1 yes) signal from the leak detection sensor (100 Hz).
- `temp_res`: the resistance (Ohms) of the hull thermistor (100 Hz).
- `temp`: the temperature (C) calculated from the hull thermistor (100 Hz).
- `temp_stat`: unused.
- `AMC_SwOnRdy`: three-bit binary diagnostic from AMC motor controller. Output of 110 implies both motors are powered on (100 Hz).
- `AMC_SwOn`: three-bit binary diagnostic from AMC motor controller. Output of 110 implies both motors are powered on (100 Hz).
- `AMC_OpEnabled`: three-bit binary diagnostic from AMC motor controller. Output of 110 implies operation has been enabled on both motors (100 Hz).
- `AMC_Fault`: three-bit binary diagnostic from AMC motor controller. Output of 110 implies a fault exists on both motors. This is common prior to the motors being powered on. (100 Hz).
- `AMC_OutEnabled`: three-bit binary diagnostic from AMC motor controller. Output of 110 implies driver output has been enabled to both motors (100 Hz).
- `AMC_QuickStop`: three-bit binary diagnostic from AMC motor controller. Output of 110 implies that quick stop has been enabled on both motors (100 Hz).
- `AMC_SwOnDisable`: three-bit binary diagnostic from AMC motor controller. Output of 110 implies that power on is disabled to both motors. This is commonly 110 briefly while toggling motor power (100 Hz).
- `AMC_Warning`: three-bit binary diagnostic from AMC motor controller. Output of 000 implies that no warning is present on either controller (100 Hz).
- `AMC_Manufacturer`: three-bit binary diagnostic from AMC motor controller. Output of 000 implies that no manufacturer warning is present on either controller (100 Hz).
- `AMC_Remote`: three-bit binary diagnostic from AMC motor controller. Output of 110 implies that remote operation (e.g., from the Simulink interface) has been enabled on both motors (100 Hz).
- `AMC_TargetReached`: three-bit binary diagnostic from AMC motor controller. Output of 110 is normal (100 Hz).
- `AMC_LimitActive`: unused three-bit binary diagnostic from AMC motor controller. Output of 110 would indicate a limit switch (not installed) has been triggered on both motors (100 Hz).

  - AMC_Homed: unused three-bit binary diagnostic from AMC motor controller. Output of 110 would indicate both motors have been homed (100 Hz).
  - eCAT_Err: EtherCAT error code, zero during normal operations. See associated documentation (100 Hz).
  - eCAT_LastErr: the last EtherCAT error code that appeared. Commonly 2 during normal operation, as an during initialization several errors appear and are immediately resolved (100 Hz).
  - eCAT_State: EtherCAT state (see associated documentation). A value of 8 is normal during operation (100 Hz).
  - eCAT_DC_Err: EtherCAT error indicating a problem with the 24 V power supply. A value of 0 is normal during operation (100 Hz).
  - eCAT_MN_ClkDiff: EtherCAT diagnostic (see associated documentation) related to data integrity. (100 Hz).
  - eCAT_DCInit: EtherCAT diagnostic related to the power supply. A value of 1 is normal during operation. (100 Hz).
  - eCAT_NS_ClkDiff: EtherCAT diagnostic (see associated documentation) related to data integrity. (100 Hz).
- data.imu: This field contains data from the IMU in the DAQ box.
  - IMU_samp: the index of the IMU sample (1 KHz).
  - IMU_thx: the rotation about AXIS (degrees) (1 KHz).
  - IMU_thy: the rotation about AXIS (degrees) (1 KHz).
  - IMU_thz: the rotation about AXIS (degrees) (1 KHz).
  - IMU_wx: the angular velocity about AXIS (degrees/s) (1 KHz).
  - IMU_wy: the angular velocity about AXIS (degrees/s) (1 KHz).
  - IMU_wz: the angular velocity about AXIS (degrees/s) (1 KHz).
  - IMU_accx: the angular acceleration AXIS (degrees/s^2) (1 KHz).
  - IMU_accy: the angular acceleration about AXIS (degrees/s^2) (1 KHz).
  - IMU_accz: the angular acceleration about AXIS (degrees/s^2) (1 KHz).
  - IMU_temp: the temperature of the IMU (C, 100 Hz).
- data.bridge: This field contains the synchronization time-series generated by the OSU DAQ.
  - C_sine: a 1-Hz sine wave generated by the OSU DAQ (1 KHz).

- `C_noise`: A pseudo-random binary noise time-series generated by the OSU DAQ (1 KHz).
- `C_waveStart`: A 0 or 5 V TTL signal that is high when the wave-maker is operating.
- `t`: the time stamps of raw data files collected at 1 KHz.
- `t_fwf`: the time stamps of raw data files collected at 10 KHz.
- `t_sl`: the time stamps of raw data files collected at 100 Hz.

APPENDIX B. TEST PROCEDURES

B.1. Lifting

All lifting operations are to be conducted by HWRL. The weight of the FOSWEC v2 is listed in Table 2-1. Four lifting points are located on at the four corners of the FOSWEC v2, as shown in Figure B-1. Lifts are to be performed using an overhead gantry crane and spreader box. The FOSWEC v2 has four rated steel cable lift slings to be used in this operation.

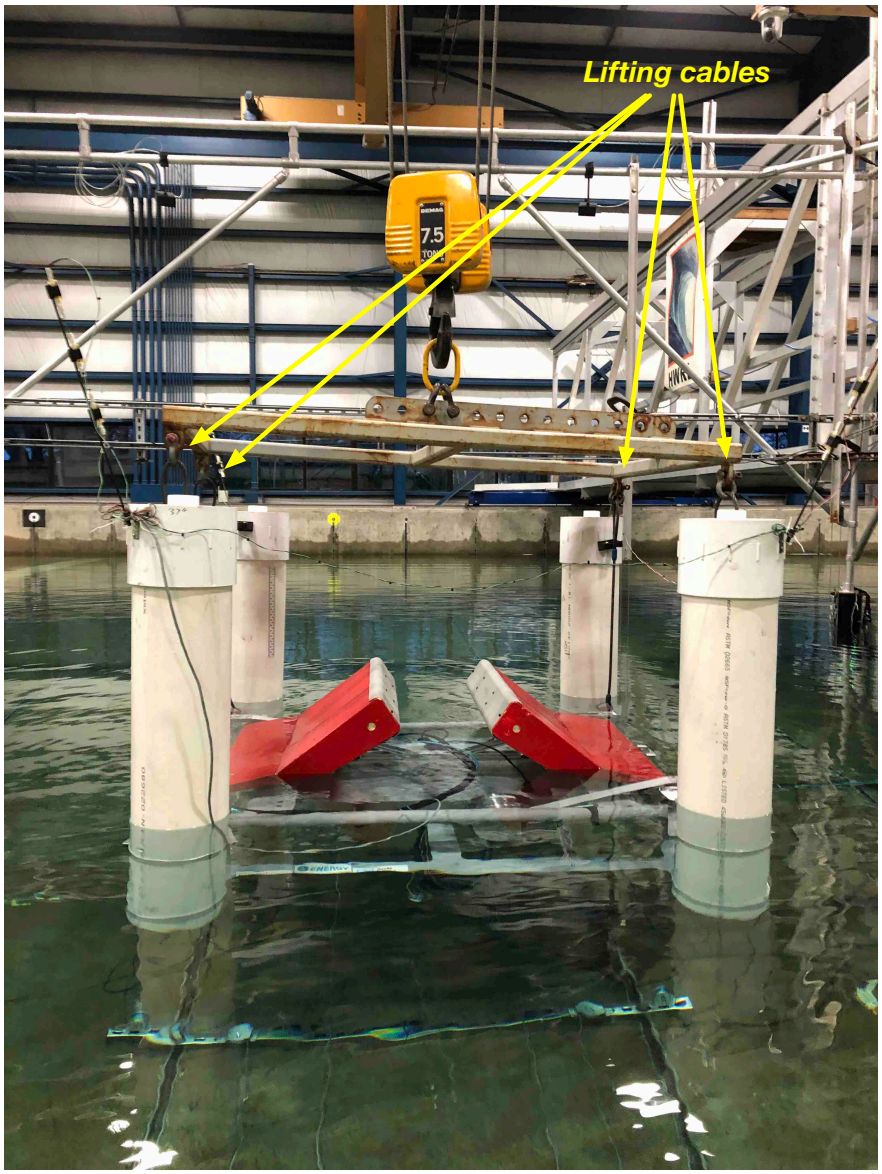

Figure B-1 Lifting cables and frame for FOSWEC v2.

B.2. Assembly

The FOSWEC v2 was assembled and underwent pre-testing at Sandia. At HRWL, the following assembly procedure was used for the FOSWEC v2.

1. Perform dry inverted pendulum (with FOSWEC v2 upside down) shakedown
    - Check FOSWEC v2 DAQ and motor functionality
    - Check linkages to HRWL DAQ (see Figure 2-5)
2. Affix Phasespace probes to FOSWEC v2
3. Prepare mooring chains and connections on basin floor
4. Connect DAQ system and power (must be done dry)
5. Lift FOSWEC into basin and make mooring connections
6. Tension mooring system (see Section 2.1.1)

B.3. Test procedure

The following test procedure was be used for the FOSWEC v2.

1. Sandia and HRWL agree on test parameters and ready respective systems
2. Sandia begins data collection
3. HRWL begins data collection
4. Wait 30 s for tare values on sensors
5. Begin test
6. Sandia gives HRWL command to stop collection
7. Sandia stops collection

B.4. Troubleshooting & disassembly

In the event of a problem, troubleshooting of the FOSWEC v2 should follow the procedures below. Note that these procedures are provided here for convenience, but official procedures are stored as ESLP forms.

- **Entering water (either by boat or directly)** - see Appendix B.4
    1. Ensure no commands are being sent to motor
    2. Disconnect 208 VAC power via blade switch using HRC 0 PPE
    3. Apply lock to disconnect switch
    4. Test disconnect via absence of voltage tester (AVT)
    5. Turn off 24 VDV power via toggle switch (optional, but best practice)
    6. Wait at least 1 time constant (75 s)
    7. Proceed with work
- **Approaching device on dry land** - see Appendix B.4
    1. (same as “Entering water”)
- **Opening FOSWEC v2 DAQ housing** - see Appendix B.4
    1. (same as “Entering water”)
- **Service of FOSWEC DC bus** - see Appendix B.4
    1. Ensure no commands are being sent to motor
    2. Disconnect 208 VAC power via blade switch using HRC 0 PPE
    3. Apply lock to disconnect switch
    4. Test disconnect via absence of voltage tester (AVT)
    5. Turn off 24 VDV power via toggle switch (optional, but best practice)
    6. Wait at least 1 time constant (75 s)
    7. Open FOSWEC v2 DAQ housing
    8. Using Class 00 gloves, measure voltage on short plug to confirm bleed resistor function
    9. Using Class 00 gloves, apply shorting key

208 VAC LOTO procedure

LOCKOUT PROCEDURE
29CFR 1910.147

Procedure #	LOTO-143028-4	**Release date:**	
Developed by:	Ryan Coe	**Location:**	FOSWEC (Roving)
Revised by:	Ryan Coe		

Equipment Identification:

Floating Oscillating Surge Wave Energy Converter (FOSWEC)

WARNING: If you must leave the equipment during this procedure, re-inspect your lock upon return to ensure your LOCKOUT has not been tampered with or removed.

This procedure covers the servicing and maintenance of machines and equipment in which the "unexpected" energization or start-up of the machines or equipment, or release of stored energy could cause injury to employees. Authority: MN471022; 29CFR1910.147.c.4

SCOPE/PURPOSE OF THIS PROCEDURE:

This procedure covers the servicing, maintenance, and implementation of updates to the FOSWEC but does not include work on the DC bus. The DC bus terminals are finger safe. Refer to ESLP procedure LOTO-163412-26 for work on the DC bus.

Select all of the following hazardous for the system covered in this procedure.

Electrical Hazard Details

Voltage: 208 volts AC or DC? AC

Mechanical Hazard Details

Pinch/crush/debris from moving flaps, belts, and gears

AUTHORIZED AND AFFECTED WORKERS

Is this a Group LOTO?

Primary Authorized Worker: Ryan Coe

Method of Energy Control: Individual Locks Applied to All Isolations

Authorized Workers

List the names and details of the authorized workers for this procedure.

Name	Org	Email
Giorgio Bacelli	08822	gbacell@sandia.gov
Dominic Forbush	08822	dforbus@sandia.gov
Kevin Dullea	06533	kjdulle@sandia.gov
Steven Spencer	06533	sjspenc@sandia.gov
Ryan Coe	08822	rcoe@sandia.gov

LOCKOUT PROCEDURE
29CFR 1910.147

Affected Workers			
Specify affected workers by area/location, list the affected area/location below.			
Site	**Bldg**	**Room**	**Notes**
NM	6970	N/A	Shared high-bay workspace

SHUTDOWN AND ISOLATION

Shutdown the Equipment

Select applicable option for shutdown instructions.

Ensure no commands are being sent to motor controllers (stop Simulink model, Driveware, and EtherCAT Configurator).

ISOLATION

Note: List isolation points in order

Source	Isolation Point (Location)	Device Type	Visual Reference	Confirm Confirm Application of Lock/Isolation
Electrical>50VAC, 100VDC	Blade switch on disconnect box (see photo).	Circuit Breaker Lockout	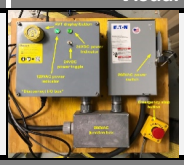	☐ *Check when applied*
	Method/Required Position			
	Move blade switch to "off" position while wearing HRC0 PPE; apply lock to disconnect switch; if performing group LOTO, use hasp			

BLOCK STORED ENERGY

Block these parts/remove linkages:

RELEASE STORED ENERGY

Note: List release points in order.

Source	Release Point (Location)	Release Component	Visual Reference	Confirm Application of Lock/Isolation
				☐ *Check when applied*

LOCKOUT PROCEDURE
29CFR 1910.147

	Method/Required Position

ZERO ENERGY VERIFICATION

Electrical Equipment

Select applicable option for shutdown instructions

Zero Voltage Verification Process

1. Perform Shock and Arc Flash Hazard Analysis:
   - Limited Approach boundary: 42" inches
   - Restricted Approach boundary: 12" inches
   - Arc Flash Boundary: <18" inches
   - Shock PPE:

N/A

   - Arc Flash PPE:

208VAC switching: HRC 0 (Long sleeve cotton shirt, eye protection, hearing protection, and long cotton pants, heavy duty leather gloves)

2. Identify meter to be used in performance of verification:

Panduit Verisafe

3. Identify who will be performing the verification:

Primary Authorized Worker

4. Perform zero energy verification as follows:
   a. Attempt to start the machine/equipment. Verify equipment does not start.
   b. Physically establish approach boundary (must be physical barrier).
   c. Don PPE identified above.
   d. Test meter on known, live source.
   e. Verify zero energy on equipment by measuring voltage phase-to-phase and phase-to-ground on all
   f. Test meter on known, live source.
5. Other methods of zero energy verification (specify):

Panduit Verisafe for 208VAC

Non-electrical Equipment

For all non-electrical hazards identified in TABLE REFERENCE, verify zero energy as follows:

Hazard	Method of Verification	Required PPE

Second Zero Energy Verification

Complete second zero energy verification ***(Must be completed by another authorized worker)*** ☐

LOCKOUT PROCEDURE
29CFR 1910.147

PERFORM SERVICING OR MAINTENANCE

Perform work in accordance with servicing or maintenance instructions.

Removal of Lockout

1. Verify work is complete and work area is clear of foreign objects, tools, etc.
2. Verify personnel are clear of work area.
3. Remove locks and lockout devices on energy isolation points identified in "Application of Lockout" step 3, above.

DO NOTREPOSITION ENERGY CONTROL DEVICES AT THIS TIME.

4. Notify affected workers identified in "Application of Lockout" step 1.E, above.
5. Restore energy isolation devices sequentially (if applicable) and restart/energize.

Restoration Sequence Information:

Ensure any tools or shorts are removed for the DAQ housing; restore limited approach boundary; confirm no commands being sent to motor controllers; restore 208VAC power via disconnect switch

300 VDC LOTO procedure

LOCKOUT PROCEDURE
29CFR 1910.147

Procedure #	LOTO-163412-26	**Release date:**	
Developed by:	Ryan Coe	**Location:**	FOSWEC (Roving)
Revised by:	Ryan Coe		

Equipment Identification:

Floating Oscillating Surge Wave Energy Converter (FOSWEC)

WARNING: If you must leave the equipment during this procedure, re-inspect your lock upon return to ensure your LOCKOUT has not been tampered with or removed.

This procedure covers the servicing and maintenance of machines and equipment in which the "unexpected" energization or start-up of the machines or equipment, or release of stored energy could cause injury to employees. Authority: MN471022; 29CFR1910.147.c.4

SCOPE/PURPOSE OF THIS PROCEDURE:

This procedure covers the servicing, maintenance, and the implementation of updates to the FOSWEC DC Bus

Select all of the following hazardous for the system covered in this procedure.

Electrical Hazard Details

Voltage:	300	volts	AC or DC?	DC
Voltage:	208	volts	AC or DC?	AC

Mechanical Hazard Details

Moving flaps, gears, and belts

Stored Energy Details

Type:	Electrical	Location:	DC bus (2) inside DAQ box

AUTHORIZED AND AFFECTED WORKERS

Is this a Group LOTO?

Primary Authorized Worker:	Ryan Coe
Method of Energy Control:	Individual Locks Applied to All Isolations

Authorized Workers

List the names and details of the authorized workers for this procedure.

LOCKOUT PROCEDURE
29CFR 1910.147

Name	Org	Email
Giorgio Bacelli	08822	gbacell@sandia.gov
Dominic Forbush	08822	dforbus@sandia.gov
Kevin Dullea	06533	kjdulle@sandia.gov
Steven Spencer	06533	sjspenc@sandia.gov
Ryan Coe	08822	rcoe@sandia.gov

Affected Workers

Specify affected workers by area/location, list the affected area/location below.

Site	Bldg	Room	Notes
NM	6970	N/A	Shared high-bay workspace

SHUTDOWN AND ISOLATION
Shutdown the Equipment

Select applicable option for shutdown instructions.

Remove device from water and ensure no commands are being sent to motor controllers (stop Simulink model, Driveware, and EtherCAT Configurator).

ISOLATION

Note: List isolation points in order

Source	Isolation Point (Location)	Device Type	Visual Reference	Confirm Confirm Application of Lock/Isolation
Electrical>50VAC, 100VDC	Blade switch on disconnect box (see photo).	Circuit Breaker Lockout	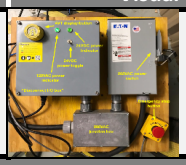	☐ *Check when applied*
	Method/Required Position			
	Move blade switch to "off" position while wearing HRC0 PPE; apply lock to disconnect switch; if performing group LOTO, use hasp			

BLOCK STORED ENERGY

Block these parts/remove linkages:

RELEASE STORED ENERGY

Note: List release points in order.

Source	Release Point (Location)	Release Component	Visual Reference	Confirm Application of Lock/Isolation

LOCKOUT PROCEDURE
29CFR 1910.147

Stored Energy	Shorting key (see photo)	Capacitors (2)	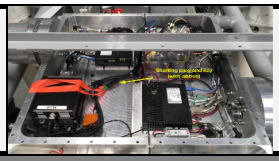	☐ *Check when applied*
	Method/Required Position			
	Wait at least 1 time constant (75 seconds) 5 time constants recommended, measure voltage on short plug to confirm bleed resistor function. Apply shorting key. (Time constant not available in manufacturer documentation, measured experimentally, per M Williams recommendation, on system 11/18/19 by R Coe, G Bacelli, S Spencer, and D Forbush.)			

ZERO ENERGY VERIFICATION

Electrical Equipment

Select applicable option for shutdown instructions

Zero Voltage Verification Process

1. Perform Shock and Arc Flash Hazard Analysis:
   - Limited Approach boundary: 42" inches
   - Restricted Approach boundary: 12" inches
   - Arc Flash Boundary: 0.4" inches
   - Shock PPE:

     Bus verification: Class 00 gloves
   - Arc Flash PPE:

     208VAC switching: HRC 0 (Long sleeve cotton shirt, eye protection, hearing protection, and long cotton pants, heavy duty leather gloves)
2. Identify meter to be used in performance of verification:

   Panduit Verisafe for 208 VAC and Fluke 117 (CAT III, rated to 600 V) for DC bus
3. Identify who will be performing the verification:

   Primary Authorized Worker
4. Perform zero energy verification as follows:
   a. Attempt to start the machine/equipment. Verify equipment does not start.
   b. Physically establish approach boundary (must be physical barrier).
   c. Don PPE identified above.
   d. Test meter on known, live source.
   e. Verify zero energy on equipment by measuring voltage phase-to-phase and phase-to-ground on all
   f. Test meter on known, live source.
5. Other methods of zero energy verification (specify):

   After confirming 208VAC is removed via Verisafe AVT, DC bus: multimeter listed above to test fo DC bus voltage drop to confirm bleed resistor function. Once 0VDC, applying a shorting key.

Non-electrical Equipment

For all non-electrical hazards identified in TABLE REFERENCE, verify zero energy as follows:

LOCKOUT PROCEDURE
29CFR 1910.147

Hazard	Method of Verification	Required PPE

Second Zero Energy Verification

Complete second zero energy verification ***(Must be completed by another authorized worker)***	☐

PERFORM SERVICING OR MAINTENANCE

Perform work in accordance with servicing or maintenance instructions.

Removal of Lockout

1. Verify work is complete and work area is clear of foreign objects, tools, etc.
2. Verify personnel are clear of work area.
3. Remove locks and lockout devices on energy isolation points identified in "Application of Lockout" step 3, above.

DO NOTREPOSITION ENERGY CONTROL DEVICES AT THIS TIME.

4. Notify affected workers identified in "Application of Lockout" step 1.E, above.
5. Restore energy isolation devices sequentially (if applicable) and restart/energize.

Restoration Sequence Information:

Ensure any tools or shorts are removed for the DAQ housing; restore limited approach boundary; confirm no commands being sent to motor controllers; restore 208VAC power via disconnect switch

APPENDIX C. TEST LOG

Test ID	Description	Notes
	FOSWEC REASSEMBLED PRESHIP TESTS	
105	ramps test	Noted Kt far off on both bow and aft; recommutate motor
106	motor autocommutated, ramps test repeated	Bow belt too tight, tension adjusted after this test
107	ramps test, final repeat	
108	damping test w/ and w/o debug mode, ramps and sine forcing in latter part	
	FOSWEC IN KIDDIE POOL	
109	multisine A bow, multisine B aft. start around 200 s	6 A for first 700 sec, amp increased to 12 around then
110	multisine B bow, C on aft, ramped up by 75 s, 12A	
111	multisine C bow, A on aft, ramped up by 75 s, 12A	
112	Above with damping. Late start due to pictures. Short test.	
	*** FOSWEC ON LAND, INVERTED, OSU BASIN***	
113		initial shakedown 2 A ramps
114	ramps for shakedown	actual shakedown, 6 A ramps
115	ramps with damping	debug mode engaged, debug limit adjusted 2 to 5 to 10 during test. Damping increased on each flap
	FOSWEC IN OSU BASIN, NO WAVES	motor encoder biases adjusted
116	throwaway ramps test, 6A max	FOSWEC sitting deeper than usual, free surface is approx at the start of float caps
117	ramps test, 10 A	FOSWEC sitting deeper than usual
118	multisine A on bow, B on aft, 12 A, ramped up by 35 s	same depth, TCP/IP timeout on stop
119	multisine A on bow, C on aft, 12 A, ramped up by 50 s	
120	multisine B on bow, C on aft, 12 A, ramped up by 35 s	
121	multisine B on bow, A on aft, 12 A, ramped up by 40 s	
122	multisine C on bow, A on aft, 12 A, ramped up by 35 s	
123	multisine C on bow, B on aft, 12 A, ramped up by 45 s	ran long intentionally to check for repeatability/basin effects
	FOSWEC IN OSU BASIN, BALLAST ADJUSTED, PHASE SPACE FRAME ADJUSTED, NO WAVE	
124	multisine A on bow, B on aft, 12 A, ramped up by 50 s	FOSWEC now sits so flap top at equilibrium is 2 in below surface
125	multisine A on bow, C on aft, 12 A, ramped up by 45 s	
126	multisine B on bow, C on aft, 12 A, ramped up by 35 s	
127	multisine B on bow, A on aft, 12 A, ramped up by 40 s	
128	multisine C on bow, A on aft, 12 A, ramped up by 40 s	
129	multisine C on bow, B on aft, 12 A, ramped up by 35 s	
130	multisine A on bow, B on aft, 9 A, ramped up by 45 s	similar runs, reduced to 9 A checkin for nonlinearities
131	multisine A on bow, C on aft, 9 A, ramped up by 45 s	
132	multisine B on bow, C on aft, 9 A, ramped up by 35 s	
133	multisine B on bow, A on aft, 9 A, ramped up by 40 s	
134	multisine C on bow, A on aft, 9 A, ramped up by 40 s	
135	multisine C on bow, B on aft, 9 A, ramped up by 40 s	
	FOSWEC IN OSU BASIN, WAVES	
136	Foswec under damping-only control gain matrix, wave R4A	wave sent for 9:20, missed the first couple of gains, gainstep 30s
137	Foswec under damping-only control gain matrix, wave R4B	wave sent for 9:20, missed the first couple of gains
138	Foswec under damping-only control gain matrix, wave R2B	controller enabled at 110s, TCP/IP Timeout error at end
139	Foswec under damping-only control gain matrix, wave R1B	controller enabled before waves
140	Foswec under damping-only control gain matrix, wave R4C	controller enabled before wavemaker start at 90s substantial rolling observed
141	ramps checkout 10A	
142	ramps checkout 10A	
143	FOSWEC under damping only control gain matrix, wave R2C	bow flap seems mostly rigid-body motion with frame, more aft excitations
144	FOSWEC under damping only control gain matrix, wave R1C	lots of mooring line snaps, TCP/IP timeout error
145	FOSWEC under damping only control gain matrix, wave R3C	lot of vibration in measured current for high damping less than 3, aft flap
146	FOSWEC under damping only control gain matrix, wave R5C	TCP/IP Timeout error. Good motion on both flaps here
147	FOSWEC under damping only control gain matrix, wave R6C	Good motion on both flaps
148	multisine A on bow, B on Aft, 9 A in pink wave H: 0.136 Phase 1	
149	multisine B on bow, C on Aft, 9 A in pink wave H: 0.136 Phase 1	bow control accidentally enabled during shutdown at end of test
150	multisine C on bow, A on Aft, 9 A in pink wave H: 0.136 Phase 1	
151	Leveling FOSWEC with TLP	Aft startboard: 8cm, aft port 9cm, aft flap: 3.5cm, bow port: 10cm, bow starboard: 8cm, bow flap: 3.5cm; PhaseSpace calibration saved
152	Ramps 10A	
153	Ramps 20A	
154	Ramps 20A	
155	ChirpC, damping: matrix (mistake)	Lateral modes at high freqs
156	ChirpC, damping: matrix (mistake)	Lateral modes at high freqs
157	multisine A on bow, B on aft, 9 A, ramped up by 35 s	

Test ID	Description	Notes
158	multisine A on bow, C on aft, 9 A, ramped up by 45 s	
159	multisine B on bow, C on aft, 9 A, ramped up by 65 s	
160	ChirpC, damping: 3	
161	Pink1C, multisine A on bow, B on aft, 9 A	air compressor came on @ 768s
162	Pink1C, multisine A on bow, C on aft, 9 A	
163	Ramps 20A	
164	multisine B on bow, A on aft, 9 A, ramped by 55s	
165	multisine A on bow, B on aft, 18 A	
166	multisine A on bow, C on aft, 18 A	
167	multisine B on bow, C on aft, 18 A	
168	multisine B on bow, A on aft, 18 A	
169	Ramps 20A	
170	Ramps 27A	disabled part way through
171	Pink1C, multisine A on bow, B on aft, 18 A	
172	Pink1C, multisine A on bow, C on aft, 18 A	
173	Pink1C, multisine B on bow, C on aft, 18 A	
174	Pink1C, multisine B on bow, A on aft, 18 A	
175	Pink2C, multisine A on bow, B on aft, 18 A	
176	Pink3C, multisine A on bow, C on aft, 18 A	wavemaker failed at 175
177	Ramps 20A	
178	Ramps 20A	
179	Pink2C, multisine A on bow, C on aft, 18 A	
180	J3C-g3.3, FOSWEC_gainMatrix_200123_104859.xlsx	Testing gain matrix, diagonals only, three 5min cycles
181	J3C-g3.3, FOSWEC_gainMatrix_200123_104922.xlsx	Testing gain matrix, all terms, three 5min cycles
182	J3C-g3.3	Unstable @ 600, stopped
183	Ramps 20A	
184	Ramps 20A	
185	multisine A on bow, B on aft, 18 A	
186	Damped (gain: 3) Ramps 20A	forgot to enable bow until partway through
	rezero motor encoders, fix mooring	
187	Ramps 20A	
188	16A bow sinusoids	started @ 20A, switched to 16A and then did low freqs again at 16A
189	9A bow sinusoids	
190	18A aft sinusoids	
191	multisine C on bow, multisine A on aft, 18 A	two cycles
	rezero motor encoders	
192	R6C, FOSWEC_gainMatrix_200124_155653	unstable @ 90s
193	R6C, FOSWEC_gainMatrix_200124_162257	
194	R5C, FOSWEC_gainMatrix_200124_162257	
195	Ramps 20A	shut off 208VAC part way through
	*** FEB 3 2020 ***	foam fell out of SW upright. Went back up when device lowered
196	Ramps 20A	TCP timeout error on termination.two test numbers before this are to level TLP w/ IMU signal and a bad ramps (came up on reference signal too late)
197	MS C on bow, A on aft, 18 A	ramped up by 30 s, terminated 360s. Occasional ringing at mid frequencies (?) in belts?
198	MS C on bow, B on aft, 18 A	ramped up by 35 s 360s
199	MS B on bow, A on aft, 18 A	ramped up by 35 s terminated 360
200	MS B on bow, A on aft, 9 A	ramped by 40 s terminated 640s for comparison to 164
201	MS C on bow, A on aft, 9 A	TCP IP timeout on termination, ramped by 40 s
202	MS C on bow, B on aft, 9 A	ramped up by 25 s
203	pink 2Cn MS C on bow, A on aft, 18 A	ramped up by 40 s , wavemaker on at 40 sec, first visible wave affect 65 s, shutdown at 800 s
204	pink 2Cn MS C on bow, B on aft, 18 A	ramped by 35, wavemaker on at 40 sec, great footage 110 - 120s. Notable mid frequency content in belts especially pronounced. Shutdown 690 s
205	pink 2Cn MS B on bow, A on aft, 18 A	ramped up by 30s, wave maker on at 40 s shutdown at 700
206	IMU levelling	no bow load cell
207	ramps demo	lost bow load cell?
208	ramps demo repeat	again no load cell
209	ramps demo repeat	earlier model from this morning loaded, still no bow load cell
210	ramps demo repeat	still no load cell
	*** Power cycled device ***	
211	captured power up and then ramps	still no load cell
212	MS C on bow, A on aft, 18 A, demo	
213	MS C on bow, B on aft, 18 A, demo	
214	MS B on bow, A on aft, 18 A demo	
215	MS C on bow, A on aft, 18 A, pink 2C	ramped up by 50 s waves on by 70, affect device by 100, 1200 s run
216	MS C on bow, B on aft, 18 A, pink 2C	
217	ramps 20A	

Test ID	Description	Notes
	*** Pulled FOSWEC TO CHECK BOW LOAD CELL CONDITION***	
	FOSWEC REDEPLOYED	
218	Ramps 20A	
	*** BOW MOTOR ENCODER OFFSET ADJUSTED ***	
219	Ramps 20A, E-stop engaged at 230 s.	only the bow flap is shut off
220	R1C gain matrix 200124_162257	controller enabled 45 s waves not till 100
221	R2C gain matrix 200124_162257	controller enabled 20 s waves 40
222	Chirp Kd only both: 1.5	controller enabled 15 s waves 55
223	JONSWAP J3C-g3.3 gain matrix 200124_162257	gain steps are 5 min and test only 15, not super useful
224	no 208V, ran white noise case to look at command amplitudes	same seed on noise commands bow/aft
225	ramps 20A	
226	0.5 ref gain white noise, changed to 0.75 ramped by 100s	seed on bow changed to 23320, aft still 23341
227	gain matrix 200205_104000 30 s step wave R1C	waves hit at 45. lateral modes in basin at this frequency. One hour run. TCP/IP timeout error at termination
228	gain matrix 200205_104000 30 s step wave R4C	waves hit at 45
229	J1C_g3.3 gain matrix 200205_10400 180 s step	waves start 40. big wave 180s, possibly maxed aft flap out 2500 lost phase space LED battery 11500 double-check formatting/timestamps for alignment
2291	ramps 20A	
230	ramps 20A	bow motor encoder about 2 pi off, perhaps initialization issue in unwrapping function? (but always on bow?)
231	check gain matrix loaded properly, check bow encoder	
	BOW MOTOR ENCODER OFFSET ADJUSTED	
232	J4C_g3.3 gain matrix 200206_095800	recorded from gain 29 till 31, mostly intended to capture gain 30
233	J4D_g3.3 gain matrix 200206_145500	breaking waves, some slapping against uprights
234	R4D with low damping only gain matrix 200206_171900.xlsx	waves 40 almost some overtopping of pipes
235	20 A ramps	
236	20A ramps	
237	J3C_g3.3 3dof gain matrix 200207_094600	data dropouts waves at 110s, double check wave repeat time
238	J2C_g3.3dof gain matrix 200207_094600	
239	Pink 2C msC on bow, msA on aft 9A	
240	Pink 2C msC on bow, msB on aft 9A	TCP/IP timeout errors
241	Pink 2C msB on bow, msC on aft 9A	
242	Pink1C msB on bow, msC on aft 9A	see test 161 and 162 for compare
243	20A ramps	
244	20A ramps	mooring not locked, check aft flap encoder, bow encoder signal off by 2pi, power cycling seemed to fix
245	20A ramps	
246	R3C gain matrix 200207_094600 30s	
247	J5Cg_3.3 gain matrix 200207_094600 180s	lost connection 2230s
248	R5C, FOSWEC_gainMatrix_200124_162257, off diagonals	error gains only changing every 3 min, wanted 30 s
249	R5C, FOSWEC_gainMatrix_200124_162257, off diagonals, 30 s gain step	went unstable but debug mode in 10A limit saved the day
250	20 A ramps	to check for any problems, aft flap encoder again shows potential problems
251	R5C, FOSWEC_gainMatrix_200124_162257_2, off diagonals, 30 s gain step	halved the diagonal spring terms, still went unstable
252	20A ramps	final test, also to check if things ok

APPENDIX D. SOFTWARE

The data acquisition and real-time control of the FOSWEC v2 relies on an EtherCAT network. A diagram of this network is shown in Figure 2-5. While this system can, in general, be controlled via any EtherCAT master, a Simulink Real-time master has been designed for the body of work described in this report. The Simulink model can be deployed to a real-time target, such as a Speedgoat.

The FOSWEC v2 motors are controlled via AMC DPEANIU-040A400 motor drives (see Figure 2-5). These controllers operate via an EtherCAT fieldbus. Additionally, for debugging and configuration, the drives can be accessed via USB and a proprietary software ("Driveware"). The key parameters that are set within Driveware are listed in Table D-1.

Table D-1 AMC motor drive settings.

Parameter	Value
Operation mode	"Profile torque" (ID 4)
Current gain, Ki	0.25
Current gain, Kp	2.25

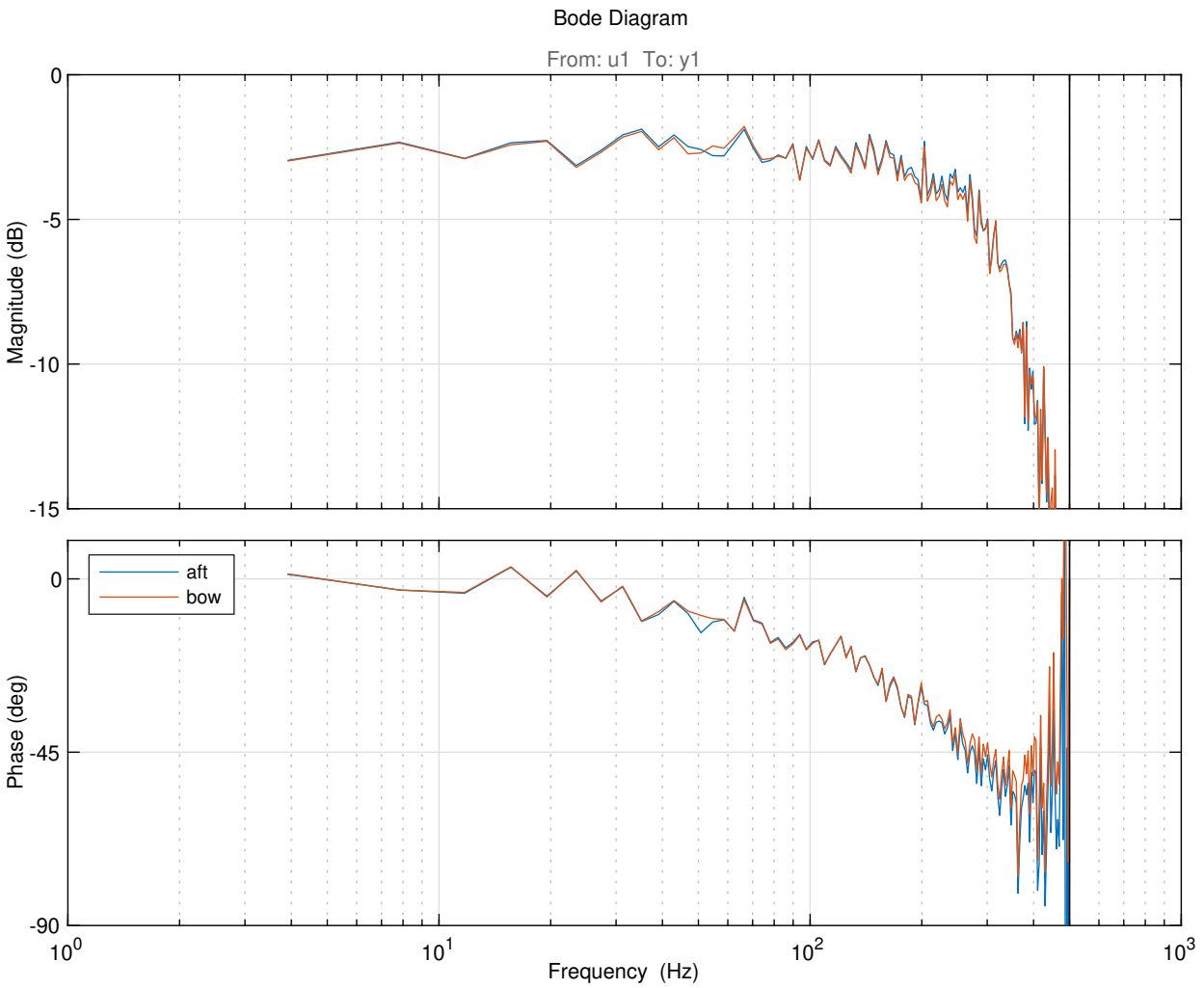

Figure E-1 Motor current commanded to measured system.

APPENDIX E. BENCH TESTING

A series of bench tests were conducted prior to wave tank testing to confirm the functionality of the FOSWEC v2's control and data acquisition systems. These tests included three basic test configurations, which are described in the following sections: a weighted pendulum test, an inverted flap test, and pool testing.

E.1. Motor current tracking

Figure E-1 shows a Bode plot describing the input-output behavior of the motor current commanded to measured system. This plot is based on an experiment using using white noise as the control input. As shown, the motor controller is capable of accurately tracking current commands up to roughly 10 Hz. At 100 Hz, the phase delay is 17.5°.

E.2. Weighted pendulum

Figure E-2 shows a photograph of a simple pendulum style test setup. This arrangement provides the most basic test of the motors functionality by removing the belt drive train. Additionally, a 50 Nm torque transducer (Futek TRS300) was connected to the motor shaft and a support bearing was added to allow a weighted pendulum to be connected to the shaft. A plate weight can be attached to the pendulum at a radius of roughly 42.2 cm.

E.3. Inverted flap

Similarly to the inverted pendulum test described in Section E.2, an inverted flap test was conducted to test the complete FOSWEC v2 drive train. In this configuration, the FOSWEC v2 is tested in its full test configuration (i.e., the drive train and DAQ system are exactly as tested in the wave tank). To provide a stable system, the FOSWEC v2 is flipped upsidedown, so that the flaps hang as pendulums. Figure E-3 shows a photo of the this configuration.

E.4. Pool test

Prior to wave tank testing, the FOSWEC v2 was tested in a small pool (7 ft wide $\times$ 10 ft long $\times$ 54 in deep; $2.13 \times 3.05 \times 1.37$ m). A photo from these tests is shown in Figure E-4. This test served

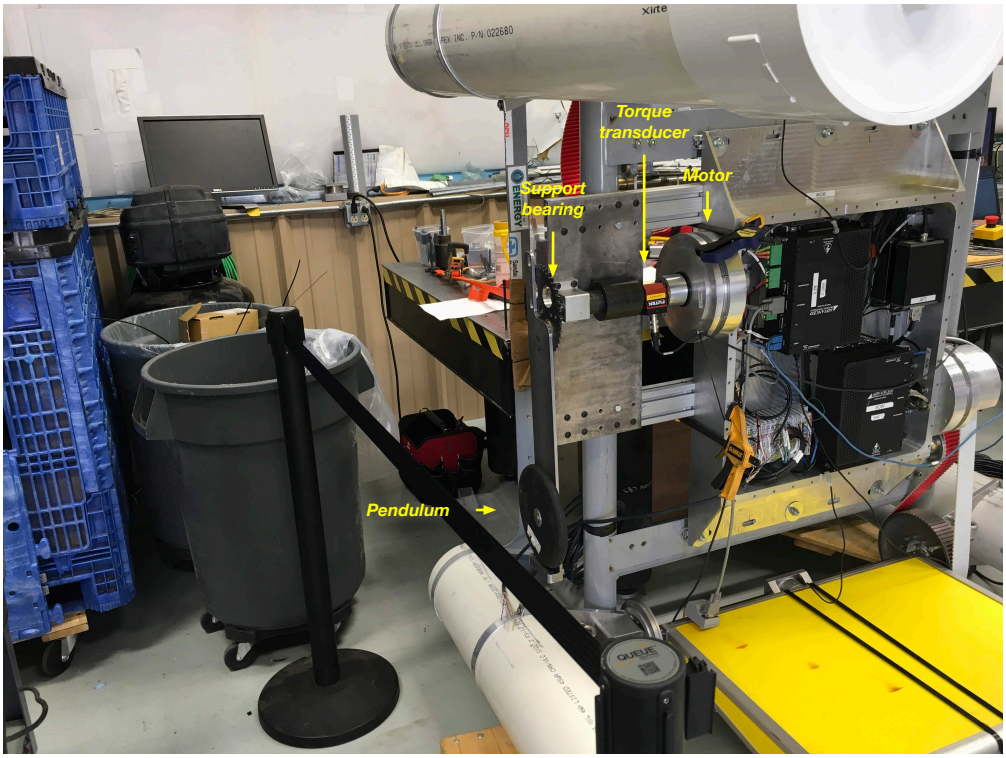

Figure E-2 Bench test set up for pendulum tests.

Figure E-3 FOSWEC v2 in inverted flap configuration.

Figure E-4 Photos of FOSWEC v2 pool test.

a number of purposes. At a basic level, this test confirmed that the FOSWEC v2 was watertight. Additionally, some work to refine the ballasting approach for the device was done during this test.

Finally, some SID tests were conducted in the pool to obtain a initial estimate of the wave-body interaction dynamics of the FOSWEC v2. It was assumed that the results of these SID tests would be badly effected by reflections from the nearby walls of the pool. The resulting impedance function of the FOSWEC v2 is shown in Figure E-5. The upper left set of plots (i.e., the 1, 1 element) corresponds to the effect of the aft flap on itself. Similarly, the upper right set of plots (i.e., the 1, 1 element) corresponds to the effect of the bow flap on the flap. Additionally, the real and imaginary components of the diagonal elements are shown in Figure E-6. Note that these impedances are based on the flap torque (as estimate from the motor current) and the flap velocity (as estimated from the motor encoder).

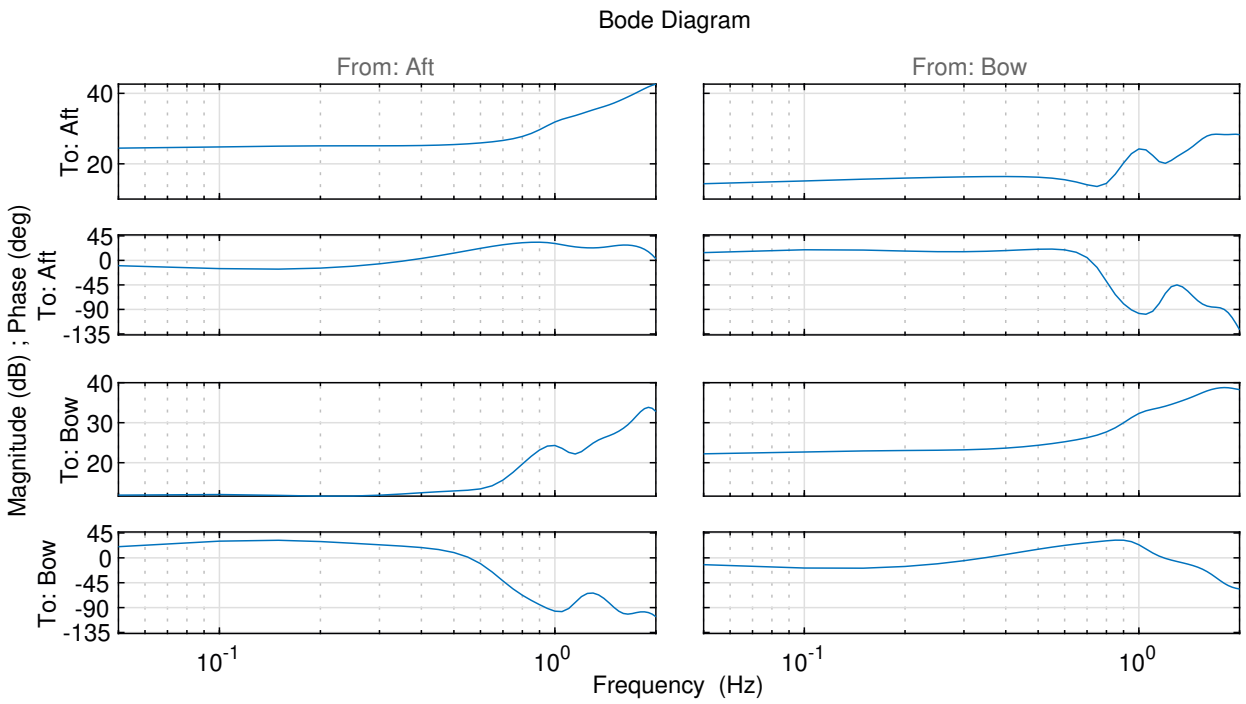

Figure E-5 Bode plot of FOSWEC v2 hydrodynamic system from "pool" test (at flap).

From Figure E-6, we can see that, for both flaps, $\Re\{Zi\} < 20$ for $f < 0.8$ Hz, which is the general range of excitation for the FOSWEC v2. Noting that this impedance is taken at the flap, and referring back to the gearings presented in Table 2-1, we can find that the required damping level at the motor is $20/3.75^2 = 1.42$ Nms/rad.

E.5. FOSWEC v2 calibration

Because the FOSWEC v2 has no direct measurement of motor torque, the following "calibration" procedure was used. This is necessary as a the relationship between the motor torque and current should remain fixed, except for the influence of belt tension and motor commutation – both of which may be subject to change. Note also that this procedure should be conducted individually for each flap.

1. **Weighted pendulum:** With the weighted pendulum connected, use a ramp test to find k_τ ($\theta = f(I) = k_\tau I$)

2. **Inverted FOSWEC v2:** Establish function between current and flap position ($\theta = f(I)$) using ramps

3. **Pool ramps:** Perform ramps in pool

4. **Experimental testing:** Proceed with experimental testing as planned

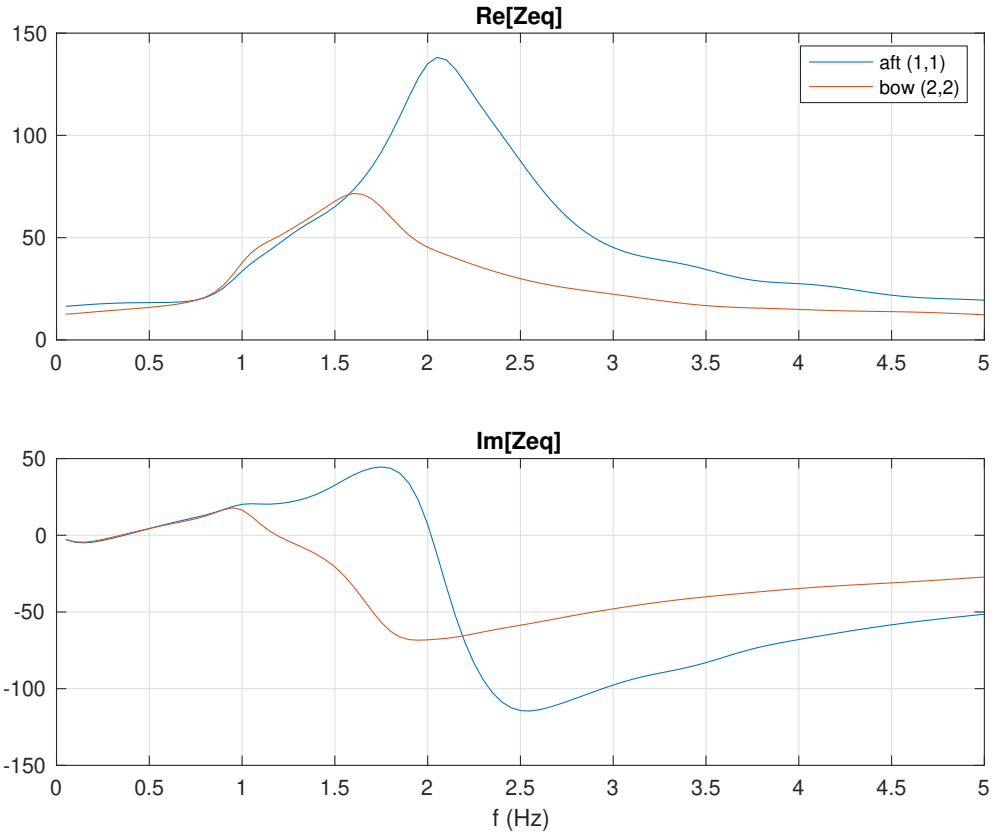

Figure E-6 Real and imaginary components of the diagonal elements of the FOSWEC v2 hydrodynamic system (at flap).

5. **Return to step 2:** (repeat step 2 to ensure that the relationship between θ and I is the same as before.)

E.6. DC discharge

A series of tests were conducted to assess the potential safety hazard posed by residual charge on the DC bus. Two variations of the test were conducted:

1. **Discharge with controllers disabled** - External power was removed from the controllers with the controllers set in disabled mode.
2. **Discharge with controllers enabled, zero command** - External power was removed from the controllers with the controllers enabled and commanded with a zero torque command.

Based on these tests, the RC time constant is 75 s. Therefore, during "off-normal events," a wait period of at least 6.25 min (5×75 s) is required before the DC bus can be considered discharged. The bridge is below the minimum voltage of 53 V at roughly 135 s. Therefore mechanical hazard can be considered eliminated also based on the 6.25 min wait period (with a safety factor of roughly 2.7).

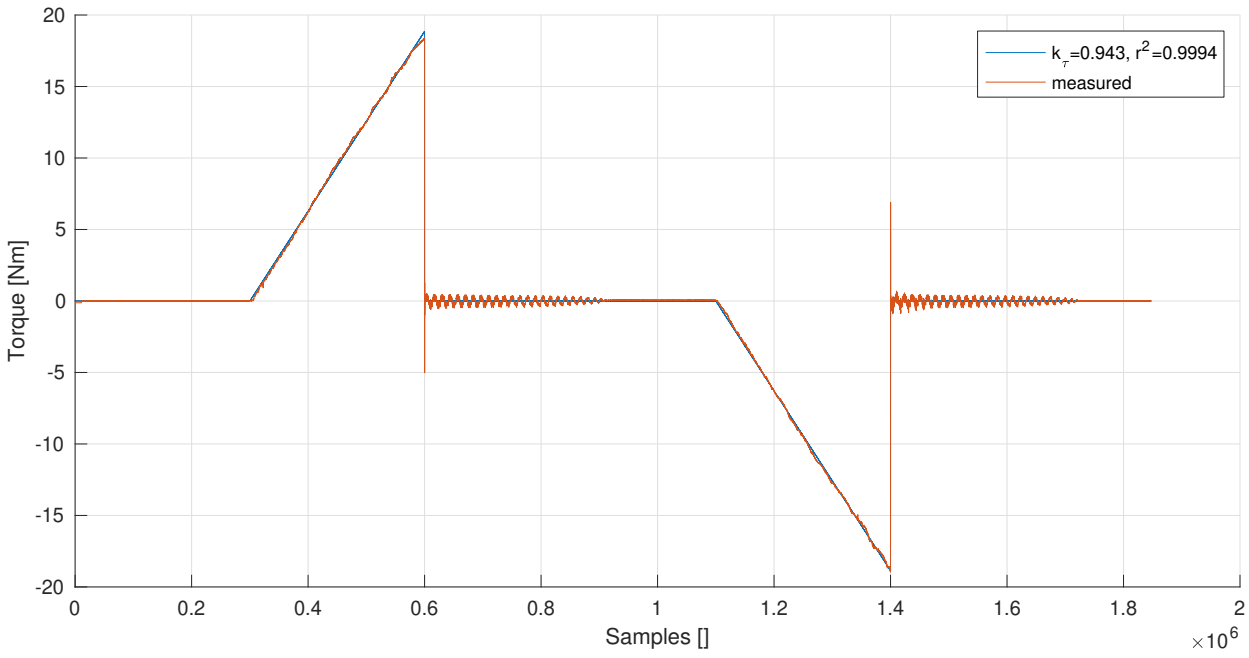

Figure E-7 Time history of ramp test with in weighted pendulum configuration to find k_τ (aft motor).

Additionally, a test was conducted to assess the potential to manual excite the flaps and charge the DC bus. In this test, the flap was disconnected and the system was manually excited by hand via the flap shaft gear. The DC bus voltage level never reached a level near 50 V. This test was considered an absolute limit, as the system would be harder to excite with the flap attached and even hard to excite in the water. Theoretically, if both motors could be excited at this rate, the DC bus could reach 71 V, but this would certainly require malicious intent and likely would not even be physically possible.

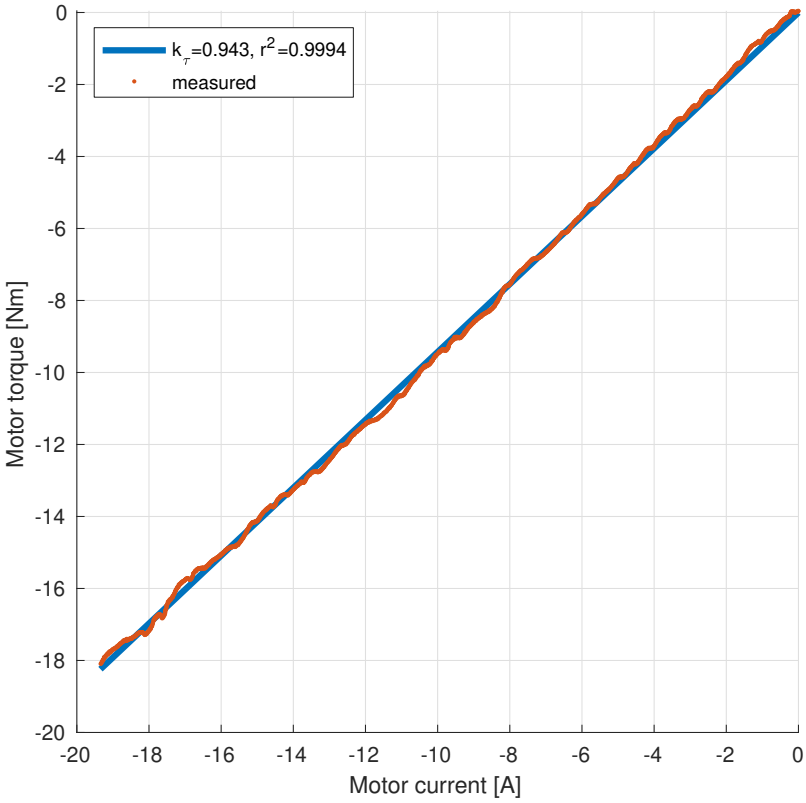

Figure E-8 Motor torque versus motor current with fit for $\tau = k_\tau I$ (aft motor).

d 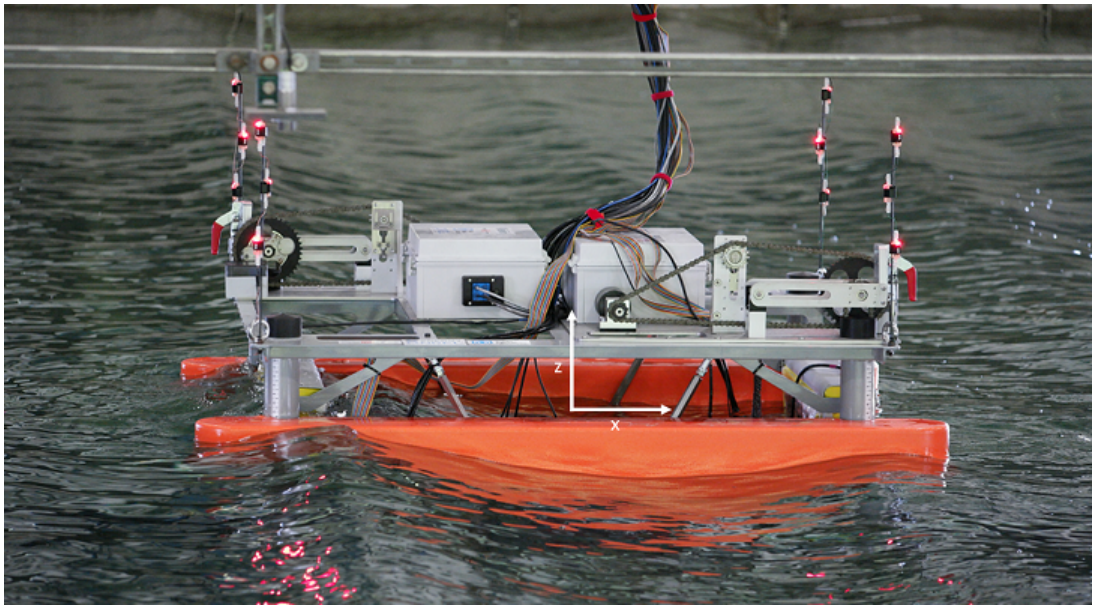

Figure F-1 FOSWEC v1 in action during "WEC-Sim" testing with origin at SWL [9].

APPENDIX F. PREVIOUS FOSWEC WORK

F.1. FOSWEC design

This section shows the previous FOSWEC design (FOSWEC v1), the basin layout used in previous tests, and results from previous tests. The FOSWEC v1 was originally conceived as a 1:33 scale device. The decision on this scale was primarily based on the wave basin dimensions and wave maker capabilities [9]. Figure F-1 shows a photograph of testing during this previous campaign. The layout of the basin, including the FOSWEC v1 device and wave probes, is shown in Figure F-2.

Figure F-3 shows the frequency response function of the FOSWEC v1's from flap based on data collected in previous testing. We can observe that the FOSWEC v1 flaps have a resonance of $\approx 0.22\,\text{Hz}$ ($T_n = 4.5\,\text{s}$).

Additionally, Table F-1 shows the operational limits distilled from previous testing. Configurations 1-4 in Table F-1 are described in Table F-2. From this, it was concluded that a motor/drivetrain cable of handling torques up to 100 Nm within $0.1 < f < 1\,\text{Hz}$ would be sufficient.

For this test, a number of substantial design updates have been made to the FOSWEC. These updates are intended to address the following issues observed in previous tests of the FOSWEC v1.

- Slack in the chain drive creates impulse loads on sensors and hysteresis.
- Some key sensors, such as the flap encoders failed or did not perform as needed.
- The configuration of the FOSWEC v1 device often created a moonpool effect.

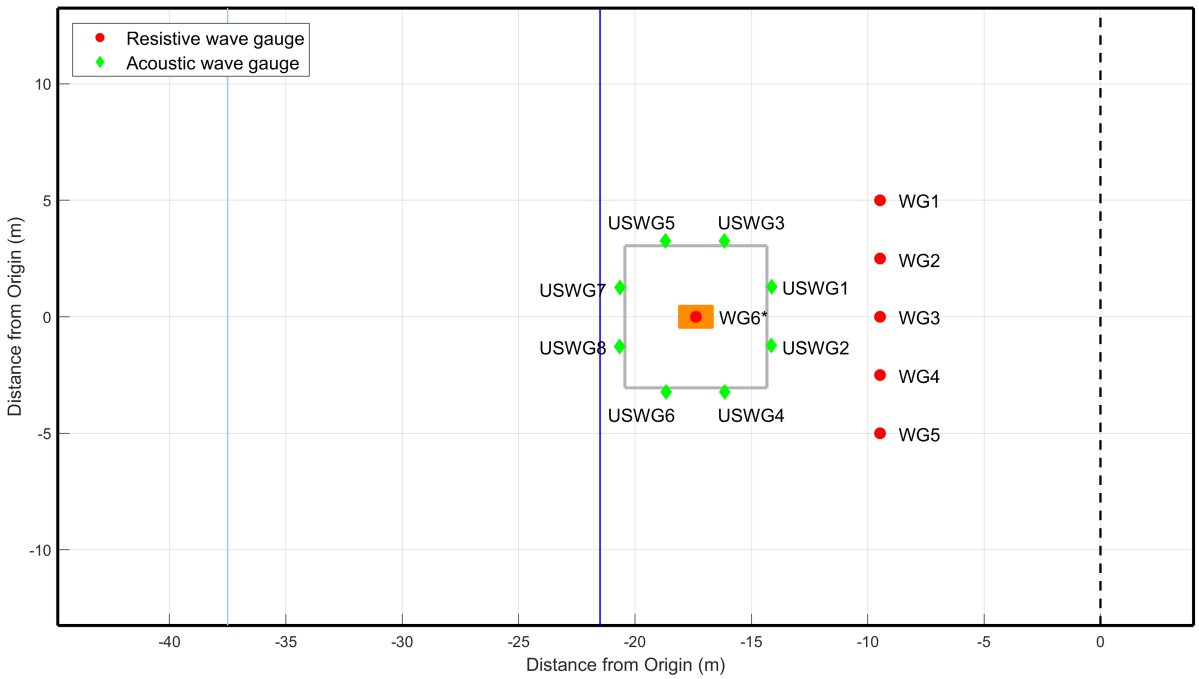

Figure F-2 DWB layout for "WEC-Sim" test. The test frame (gray) and the FOSWEC v1 device (orange rectangle). Note that wave gauge 6 (WG6) was only in place for wave calibration tests, when the FOSWEC v1 device was not in the basin. The origin is the middle of the wave maker, indicated by the dashed line. The initiation of the beach (dark blue) and the SWL (light blue) are also indicated [9].

Table F-1 Maximum operating limits based on previous "WEC-Sim" test.

Test description	Max flap torque [Nm]	Max flap displacement [deg]
Forced Oscillation	90.8	23.2
Wave Excitation	88.2	n/a
Configuration 1	68.4	24.9
Configuration 2	67.4	22.6
Configuration 3	63.4	30.2
Configuration 4	62.8	22.9

To address these issues, three areas of re-design were enacted:

- Drivetrain and motor
  - The previous chain was replaced with a Gates carbon belt.
  - The previous motors, which had a high gear ratio, was replaced with 3:1 geared Allied Motion MF0150025-C0X motors. These motors are driven with AMC DPEANIU-C100A400 motor controllers.
- Sensors

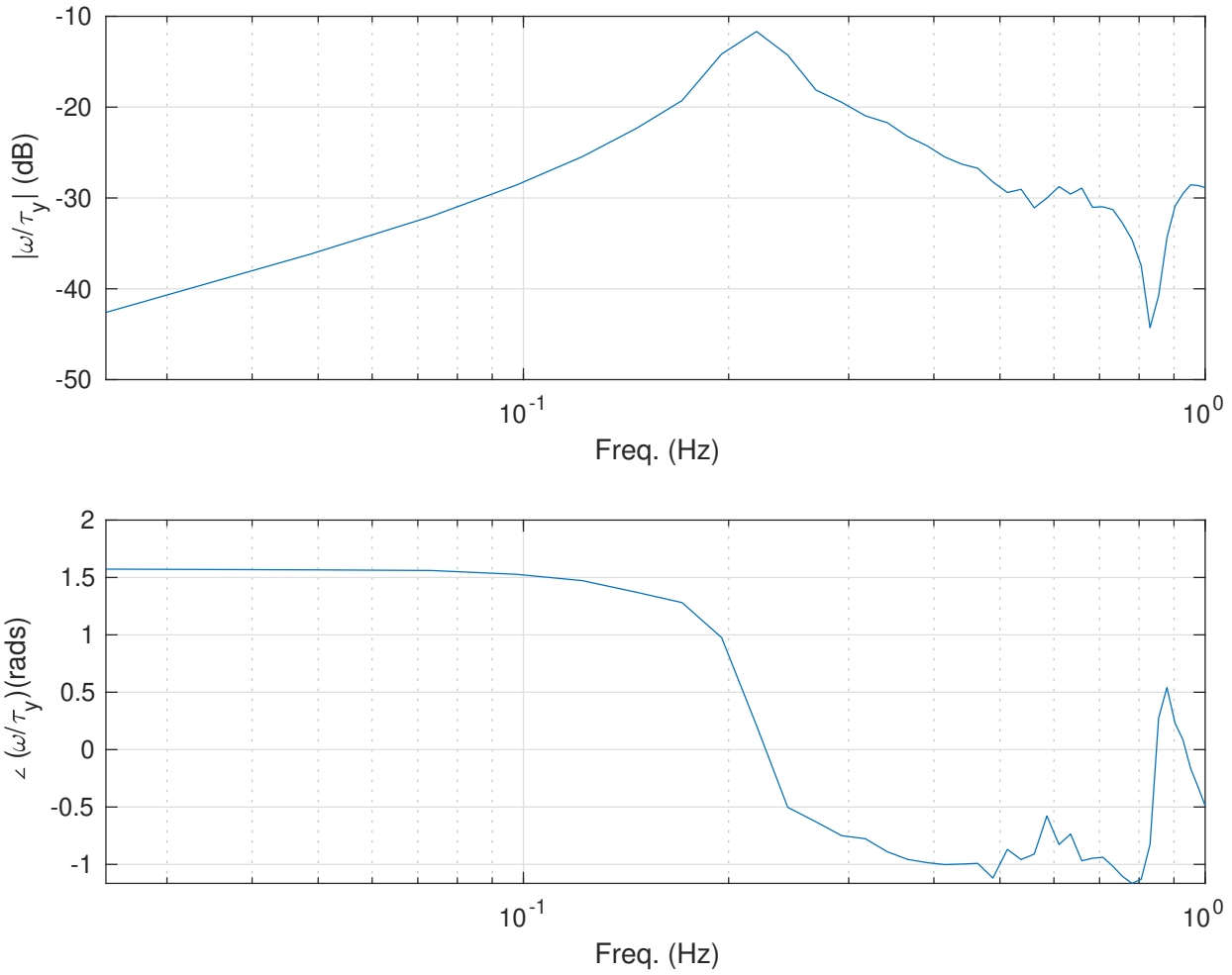

Figure F-3 FOSWEC v1 FRF from previous "WEC-Sim" testing (unpublished).

Table F-2 FOSWEC v1 configurations (Config 1 - Config 4) [9].

FOSWEC	DOF	Config 1	Config 2	Config 3	Config 4
Flap 1	Pitch (RY)	Free	Free	Free	Free
Flap 2	Pitch (RY)	Locked	Free	Free	Free
Platform	Heave (Z)	Locked	Locked	Free	Free
	Pitch (RY)	Locked	Locked	Locked	Free
	Surge (X)	Locked	Locked	Locked	Free

- The inclinometer, which did not have a sufficient bandwidth, was replaced with a Xsens 197 MTI-20-2A5G4 IMU.
- The pressure mat, which did not work reliably, was replaced by a series of Omega PX-459 pressure sensors.
- The existing Mini 9105-TW-MINI58-R-5-IP68 6DOF load cells are utilized to measure torque, but the motor current was used as the primary measurement for inferring

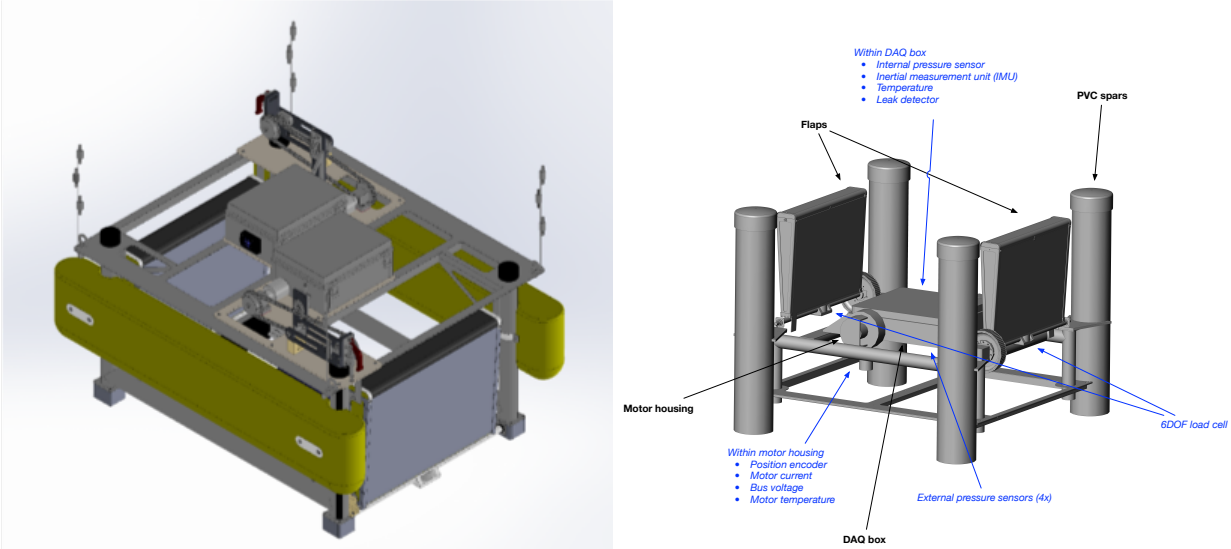

(a) FOSWEC v1 CAD from "WEC-Sim"testing. **(b) FOSWEC v2 updated CAD for current test.**

Figure F-4 FOSWEC design versions.

mechanical torque.[5]

  - Sick SKS36-HFA0-K02 Hyperface motor encoders was used.

- The pontoon flotation design, which created a moonpool effect, was replaced by a four spar "semi-submersible" design.

A comparison of the previous FOSWEC v1 design and the current FOSWEC v2 design are shown in Figure F-4.

F.2. Waves calibrated

[5]The relationship between motor current and torque was found empirically via bench testing prior to wave tank testing.

Trial	T (s)	H (m)	E_f (W/m)	T_o (s)	H_o (m)	$E_{f,o}$ (W/m)	H_o/H (-)	T_o/T (-)	$E_{f,o}/E_f$ (-)
1	0.87	0.015	0.19	0.87	0.015	0.19	1.00	1.00	1.00
2	0.87	0.045	1.72	0.87	0.044	1.64	1.00	0.97	0.95
3	1.22	0.015	0.27	1.22	0.015	0.27	1.00	0.99	0.98
4	1.22	0.045	2.43	1.22	0.045	2.36	1.00	0.99	0.97
5	1.22	0.136	21.85	1.22	0.141	23.31	1.00	1.03	1.07
6	1.22	0.242	69.05	1.22	0.237	65.90	1.00	0.98	0.95
7	1.57	0.015	0.37	1.57	0.015	0.37	1.00	1.00	1.01
8	1.57	0.045	3.32	1.57	0.046	3.39	1.00	1.01	1.02
9	1.57	0.136	29.90	1.57	0.134	28.91	1.00	0.98	0.97
10	1.91	0.015	0.49	1.92	0.015	0.49	1.00	1.00	1.01
11	1.91	0.045	4.39	1.92	0.046	4.53	1.00	1.01	1.03
12	1.91	0.136	39.52	1.91	0.135	38.70	1.00	0.99	0.98
13	1.91	0.242	124.90	1.91	0.241	123.61	1.00	1.00	0.99
14	2.26	0.015	0.60	2.26	0.015	0.61	1.00	1.01	1.02
15	2.26	0.045	5.36	2.26	0.045	5.31	1.00	0.99	0.99
16	2.26	0.136	48.25	2.26	0.136	47.84	1.00	1.00	0.99
17	2.61	0.015	0.68	2.61	0.015	0.70	1.00	1.01	1.02
18	2.61	0.045	6.13	2.61	0.046	6.19	1.00	1.00	1.01
19	2.61	0.136	55.17	2.61	0.137	55.36	1.00	1.00	1.00
20	2.61	0.242	174.37	2.61	0.246	179.91	1.00	1.02	1.03
21	3.31	0.045	7.16	3.31	0.045	6.99	1.00	0.99	0.98
22	3.31	0.136	64.48	3.30	0.138	66.01	1.00	1.01	1.02
23	3.31	0.242	203.78	3.31	0.242	202.39	1.00	1.00	0.99

Table F-3 FOSWEC v1 WEC-Sim testing regular wave calibration results [9].

Trial	T_p (s)	H_{m0} (m)	T_e (s)	E_f (W/m)	$T_{p,o}$ (s)	$H_{m0,o}$ (m)	$T_{e,o}$ (s)	$E_{f,o}$ (W/m)	$\frac{T_{p,o}}{T_p}$ (-)	$\frac{H_{m0,o}}{H_{m0}}$ (-)	$\frac{T_{e,o}}{T_e}$ (-)	$\frac{E_{f,o}}{E_f}$ (-)
1	1.22	0.015	1.07	0.12	1.12	0.015	1.06	0.12	0.92	1.01	1.00	1.02
2	1.22	0.045	1.07	1.07	1.15	0.046	1.06	1.07	0.95	1.00	1.00	1.00
3	1.22	0.136	1.07	9.61	1.28	0.110	1.17	6.91	1.05	0.81	1.09	0.72
4	2.61	0.015	2.26	0.28	2.82	0.016	2.33	0.31	1.08	1.03	1.03	1.08
5	2.61	0.045	2.26	2.56	2.48	0.046	2.26	2.65	0.95	1.02	1.00	1.04
6	2.61	0.136	2.26	23.03	2.48	0.139	2.26	23.86	0.95	1.02	1.00	1.04

Table F-4 FOSWEC v1 WEC-Sim testing irregular wave calibration results [9].

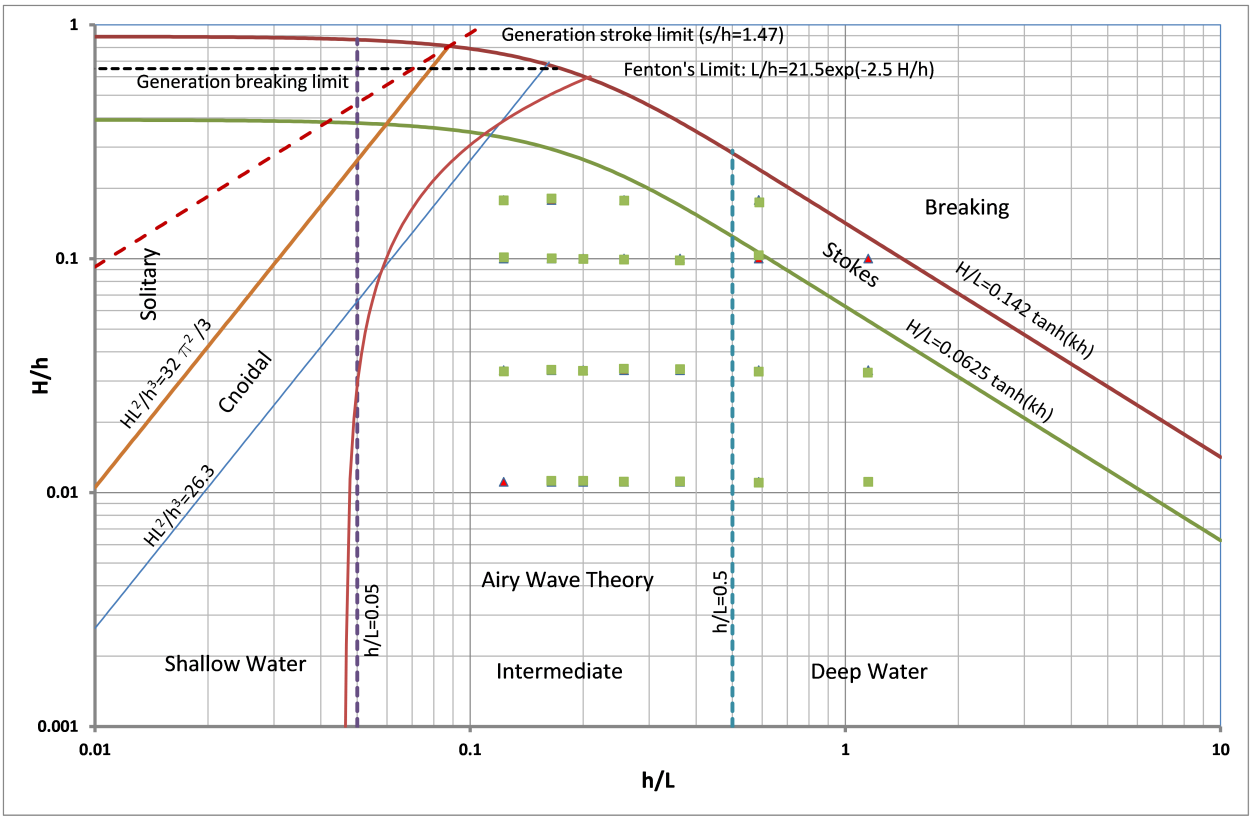

Figure F-5 FOSWEC v1 WEC-Sim testing regular wave calibration results [9].

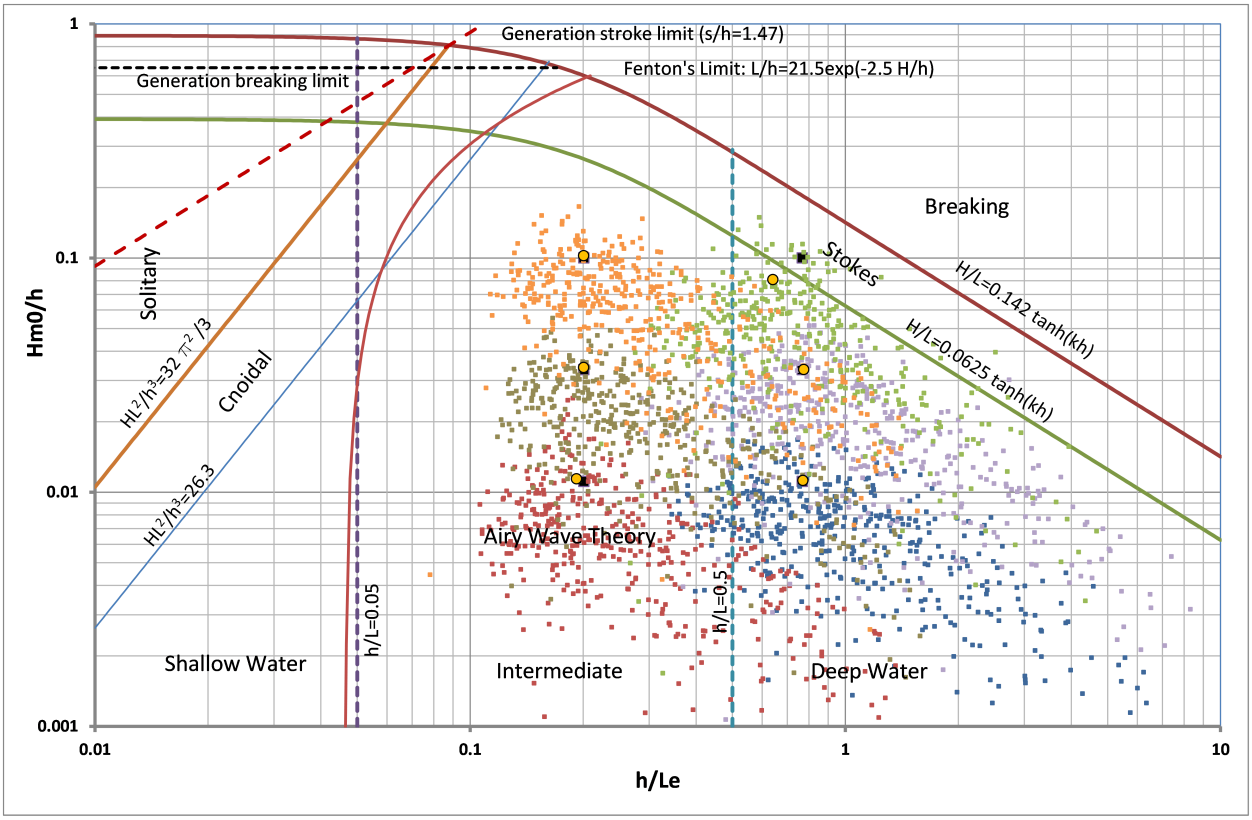

Figure F-6 FOSWEC v1 WEC-Sim testing irregular wave calibration results [9].

DISTRIBUTION

Hardcopy—External

Number of Copies	Name(s)	Company Name and Company Mailing Address

Hardcopy—Internal

Number of Copies	Name	Org.	Mailstop

Email—Internal (encrypt for OUO)

Name	Org.	Sandia Email Address
Technical Library	01177	libref@sandia.gov

Sandia National Laboratories is a multimission laboratory managed and operated by National Technology & Engineering Solutions of Sandia LLC, a wholly owned subsidiary of Honeywell International Inc., for the U.S. Department of Energy's National Nuclear Security Administration under contract DE-NA0003525.